Imaging Spectrometry of Optically-shallow Waters

Curtiss O. Davis

College of Earth, Ocean and Atmospheric Sciences, Oregon State University, Corvallis, OR 97331 cdavis@coas.oregonstate.edu

With special thanks to:

Kendall L. Carder

College of Marine Science, University of South Florida, St. Petersburg, FL 33701

Bo-Cai Gao

Remote Sensing Division, Naval Research Laboratory, Washington, D.C. 20375

Zhongping Lee

U. Mass, Boston

And many others

Imaging Spectrometry of Optically-Shallow Waters

- Why Imaging Spectrometry?
- Airborne imaging spectrometers
  - AVIRIS
  - PHILLS
  - New systems
- HICO
- Calibration
- Tafkaa Atmospheric Correction
- Optical properties and shallow water bathymetry
  - models and Inversion approaches
    - Neural networks
    - Look-up tables
    - Semi-analytical models
- Spaceborne Imaging Spectrometry
  - Hyperion Results
  - HICO results

Reminder on Hyperspectral Imaging and Linear Mixing

Hyperspectral imager

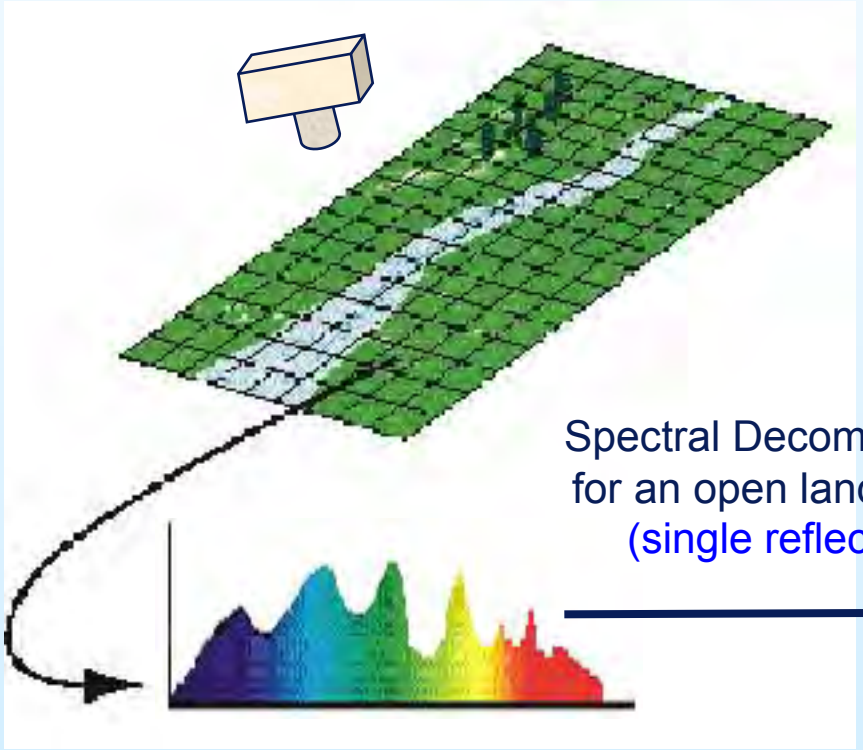

Spectrum is recorded
For *each pixel*

Spectral Decomposition
for an open land scene
(single reflection)

Linear Mixing: Subcomponents of the pixel spectrum assumed to be mixed in proportion to fractional area in pixel

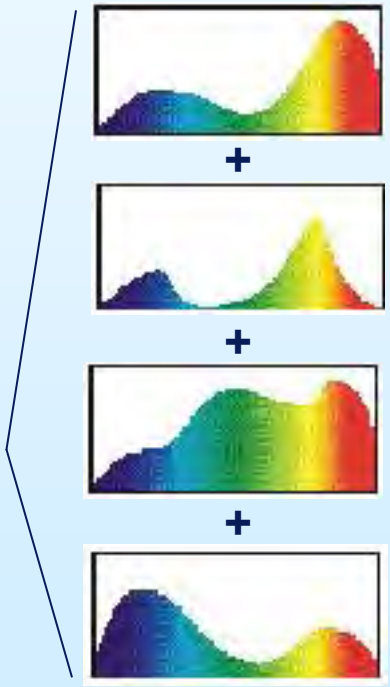

Linear Mixing techniques very successful for automated screening and cueing
And for many land applications, e.g. mineral identification

Resolving the Complexity of Coastal Optics Requires Imaging Spectrometry

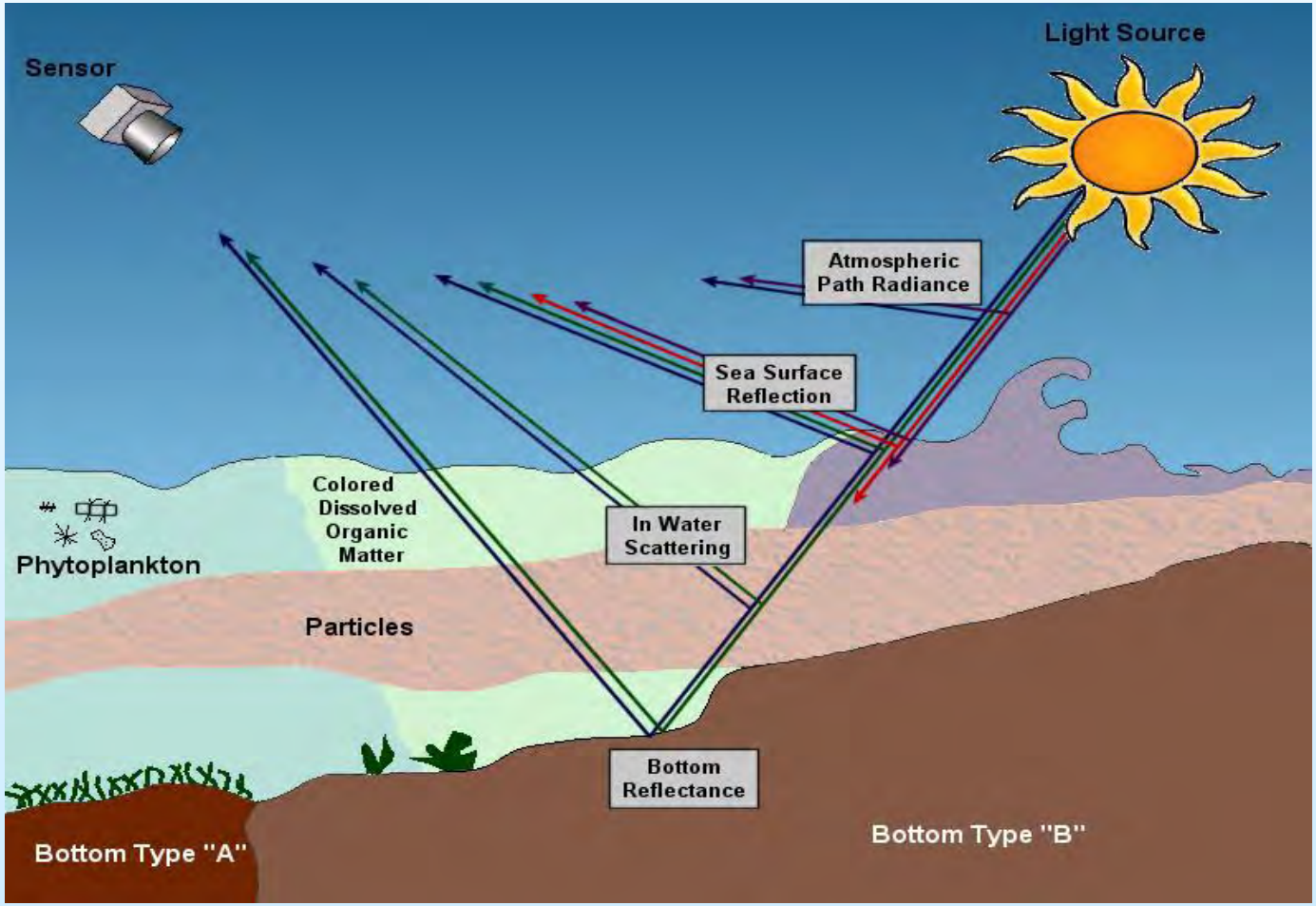

Extensive studies using shipboard measurements and airborne hyperspectral imaging have shown that visible hyperspectral imaging is the only tool available to resolve the complexity of the coastal ocean from space.
(Lee and Carder, *Appl. Opt.*, 41(12), 2191 – 2201, 2002.)

The need for High Spatial Resolution in the Near Coastal Ocean

SeaWiFS 1 km data

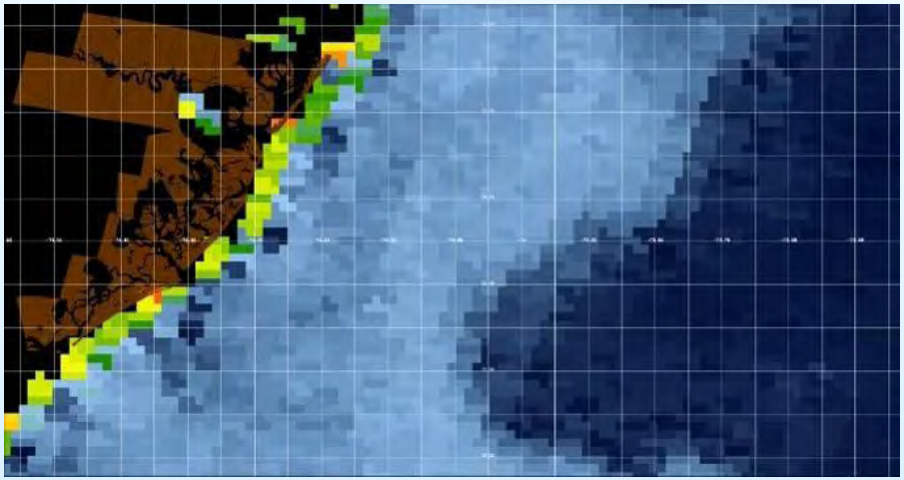

PHILLS-2 9 m data mosaic

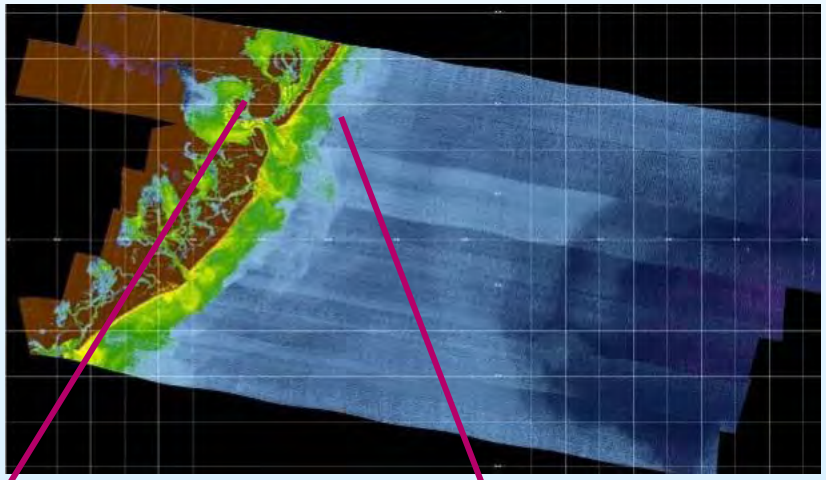

Near-simultaneous data from 5 ships, two moorings, three Aircraft and two satellites collected to address issues of scaling in the coastal zone. (HyCODE LEO-15 Experiment July 31, 2001.)

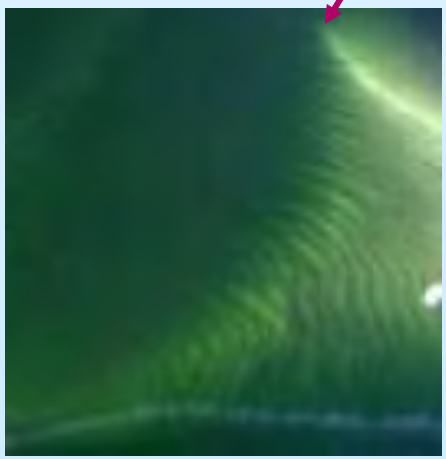

Sand waves in PHILLS-1 1.8 m data

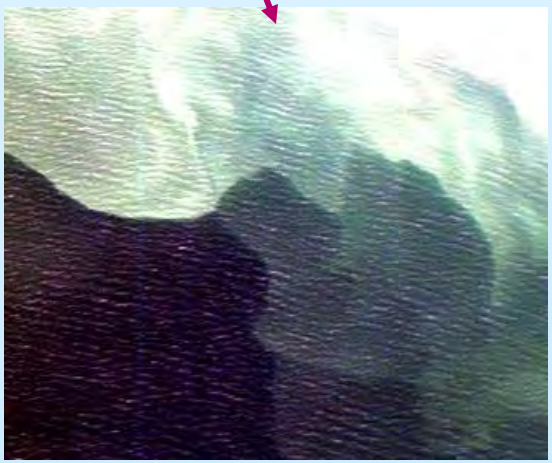

Fronts in AVIRIS 20 m data

Solving the Shallow Ocean Remote Sensing Problem using Hyperspectral Data

Remote-sensing reflectance ($R_{rs} = L_u/E_d$ *at the sea surface*) is a function of properties of the water column and the bottom,

$$R_{rs}(\lambda) = f[a(\lambda), b_b(\lambda), \rho(\lambda), H], \qquad (1)$$

where $a(\lambda)$ is the absorption coefficient, $b_b(\lambda)$ is the backscattering coefficient, $\rho(\lambda)$ is the bottom albedo, H is the bottom depth.

Where $a(\lambda)$ is the sum of $a_{water} + a_{phytoplankton} + a_{CDOM + Detritus}$

And $b_b(\lambda)$ is the sum of $b_{b\ water} + b_{b\ phytoplankton} + b_{b\ detritus} + b_{b\ sediments}$

It is desired to *simultaneously* derive bottom depth and albedo and the optical properties of the water column. This is done by taking advantage of the spectral characteristics of the absorption and reflectance characteristics of the water column constituents and the bottom.

The next three slides show examples of how bottom albedo, water optical properties and depth effect remote sensing reflectance:

Example bottom types and reflectances

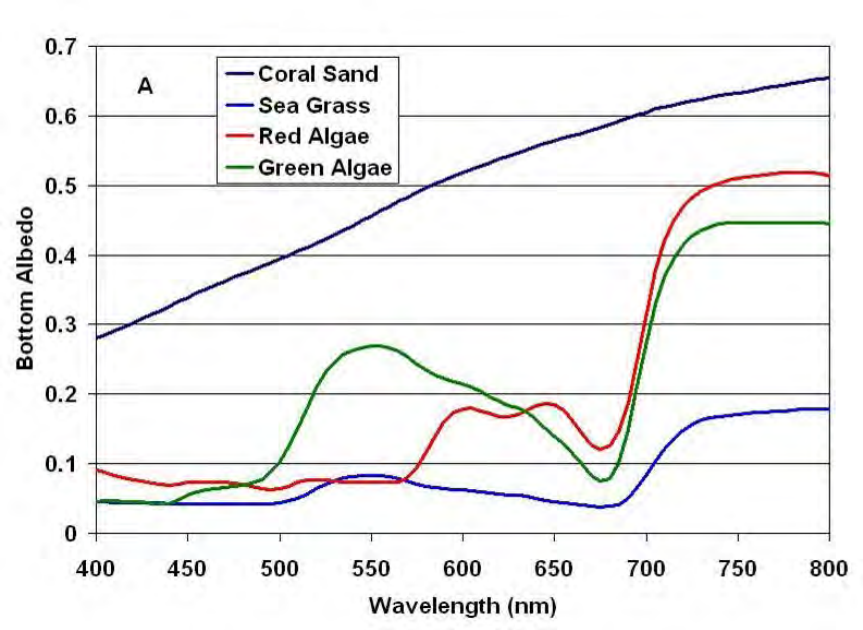

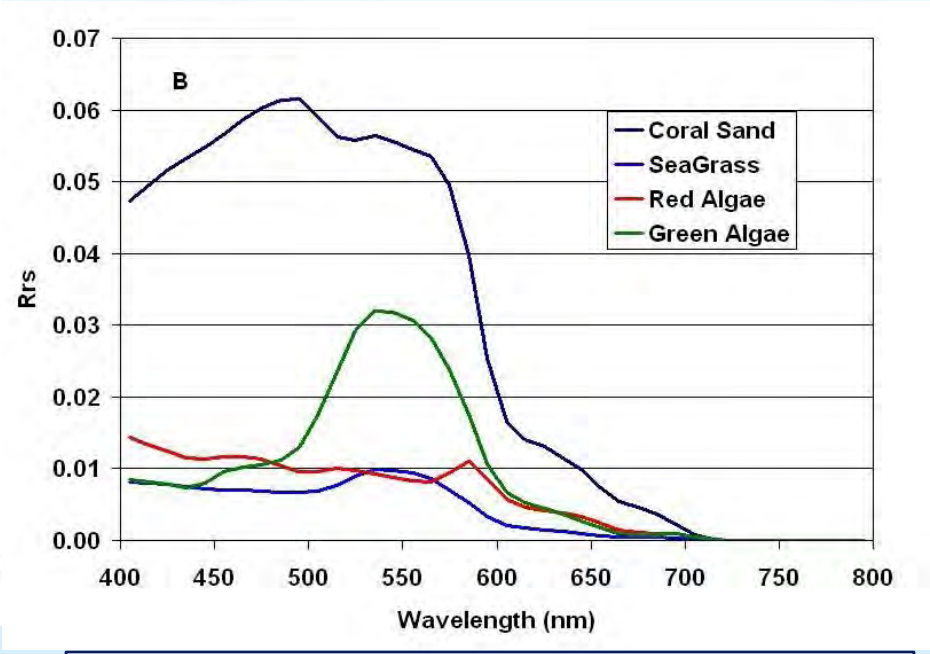

Example bottom reflectances.

Remote sensing reflectance for the Same bottom types viewed through 3 m of clear ocean water.

Curves produced using HYDROLIGHT (Curt Mobley, Sequoia Scientific, Inc.) by Bill Snyder, NRL.

Example Water Types

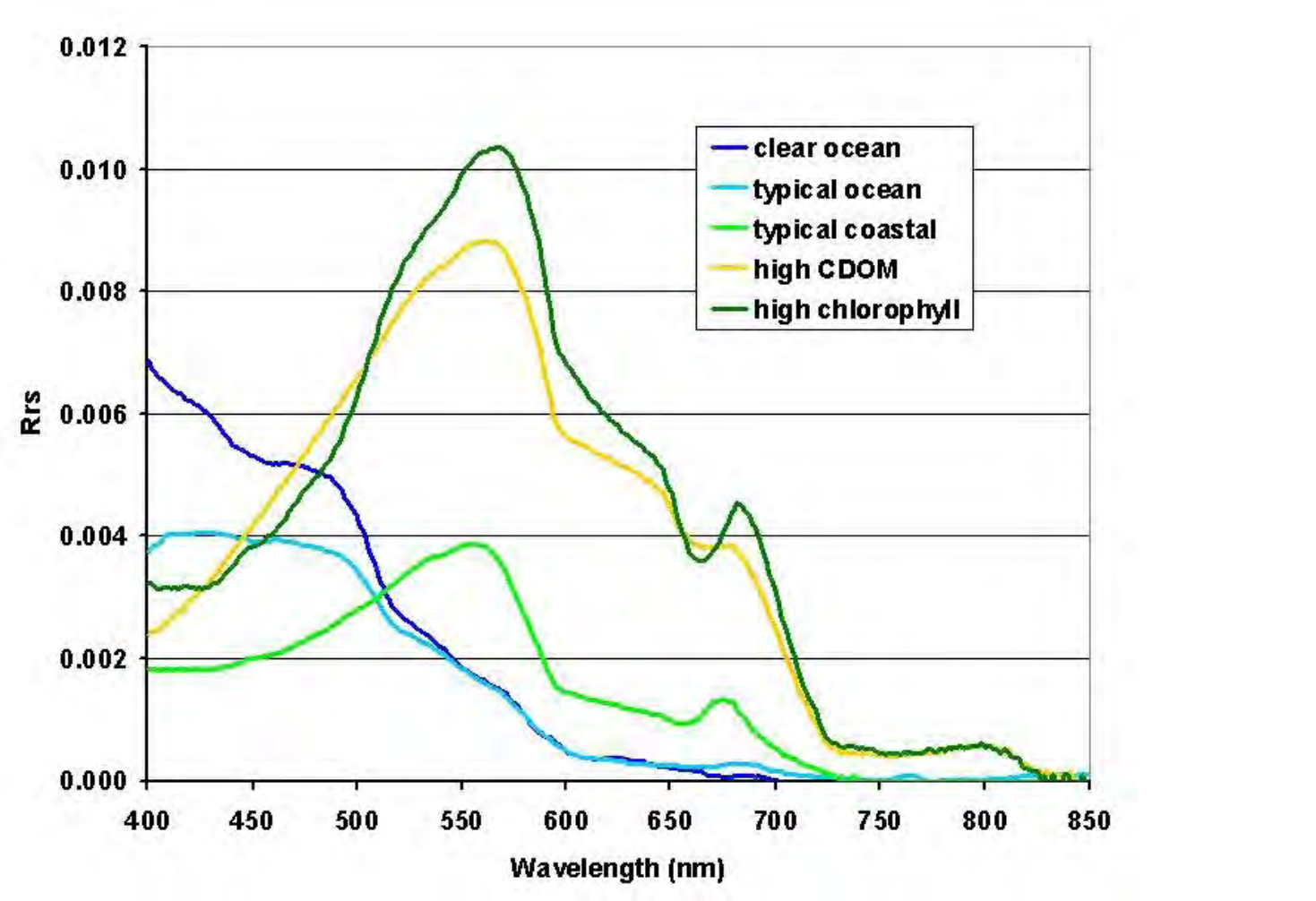

Above water remote sensing reflectances measured using an ASD spectrometer by W. Joe Rhea, NRL.

Effect of depth and water type on bottom remote sensing reflectance

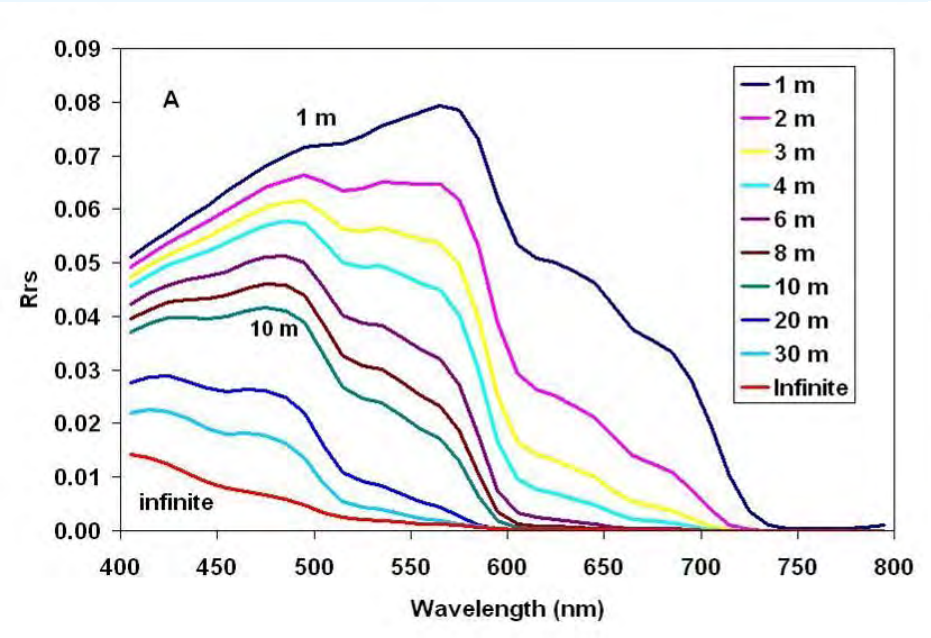

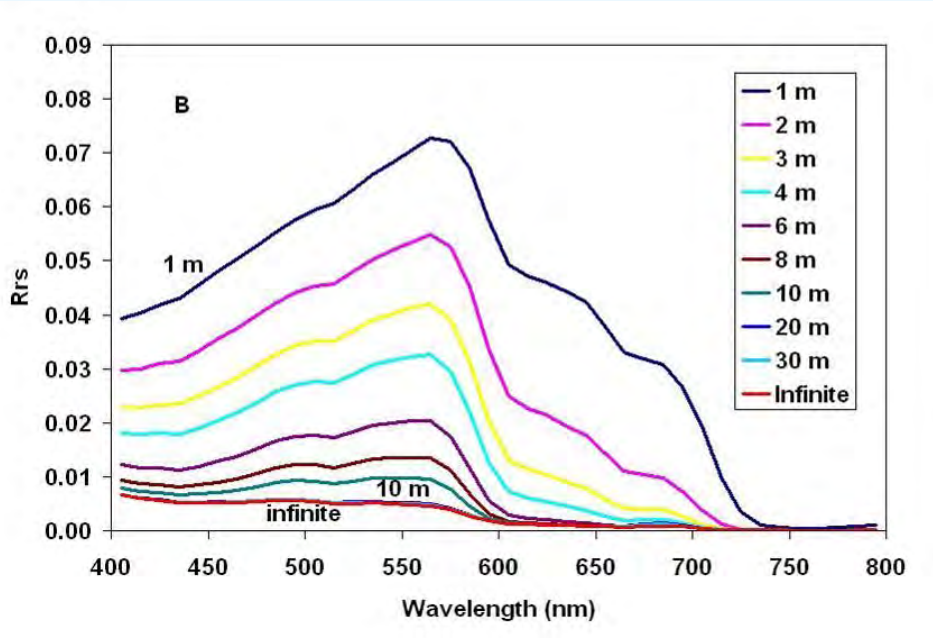

Changes in remote sensing reflectance of a coral sand bottom with depth as viewed through the clearest ocean water

Changes in remote sensing reflectance of a coral sand bottom with depth as viewed through a typical coastal water type

Curves produced using HYDROLIGHT by Bill Snyder, NRL

What we need to solve this problem

- A stable, well-calibrated sensor with high SNR
  - AVIRIS
  - PHILLS
  - SAMSON
  - CASI-1500
  - HICO
- Good Characterization and Calibration
- Atmospheric correction
- In-water algorithms to solve simultaneously for Water column optical properties, Bottom type and Bathymetry
  - Regression
  - Neural Networks
  - Look-up tables
  - HOPE

Extensive In-situ data for product validation at LEO-15 site, New Jersey, USA (HyCODE)

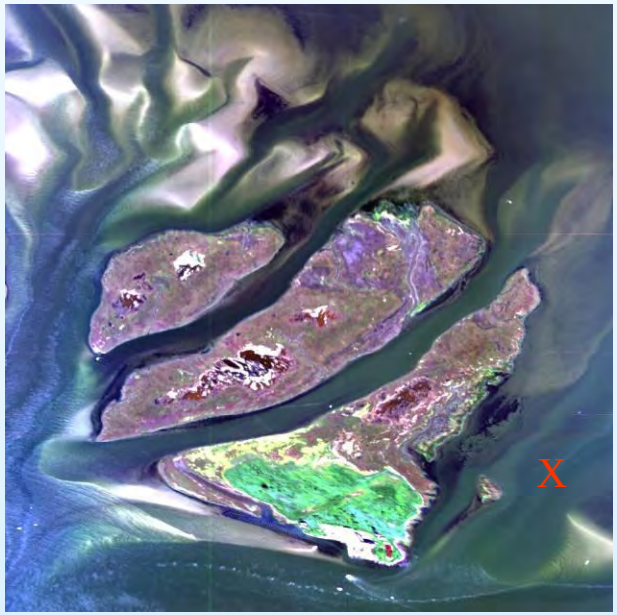

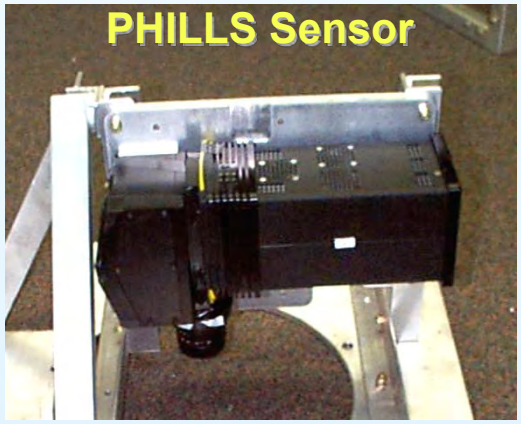

Profiling Optics and Water Return (POWR) Package

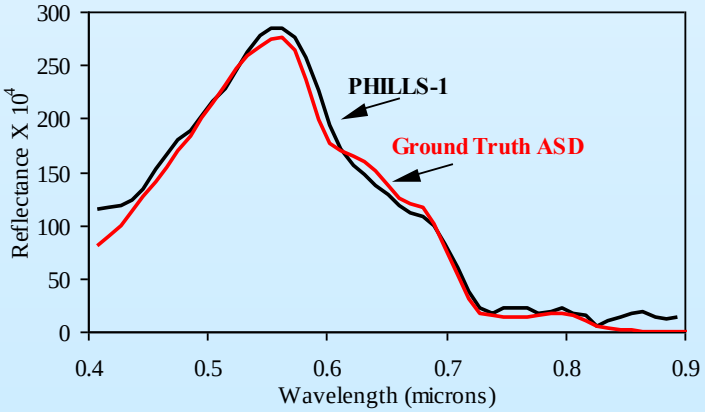

Comparison at the X. (C. O. Davis, et al., (2002), Optics Express 10:4, 210--221.)

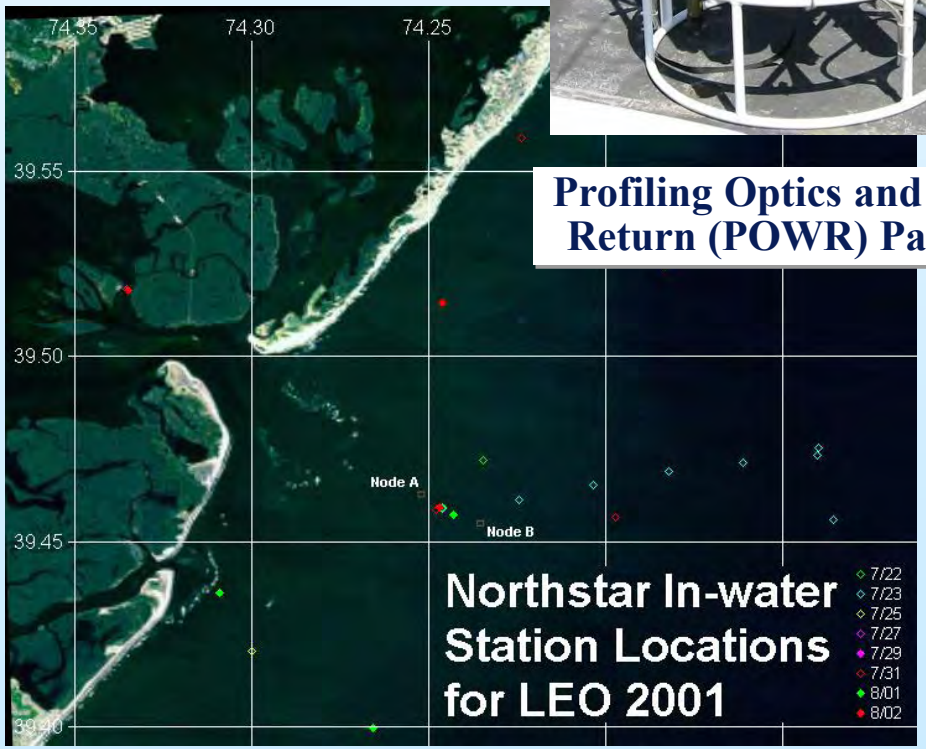

Full Spectral Atmospheric Correction

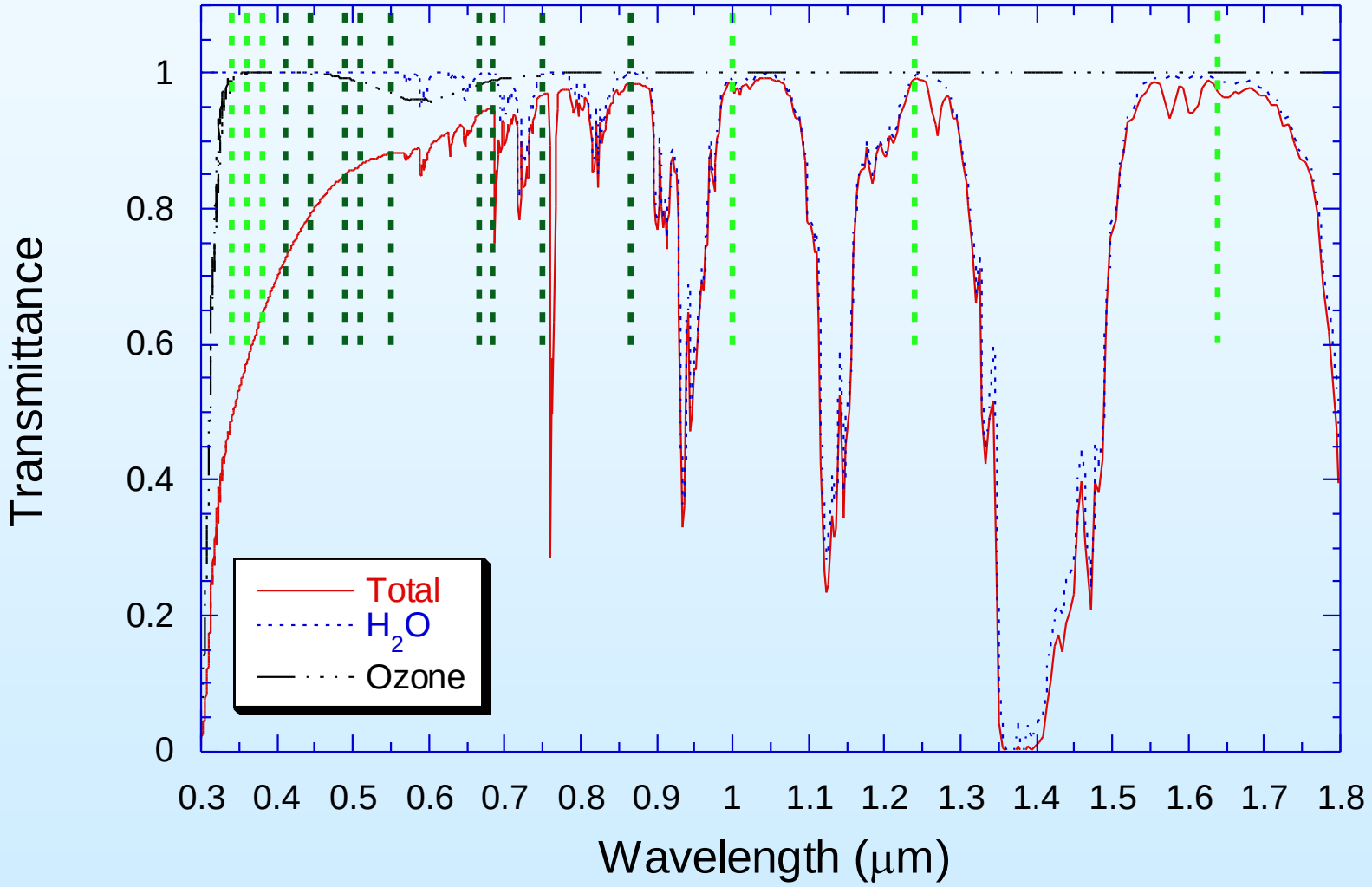

- Multispectral channels selected to avoid water vapor and other absorptions
- Must correct the full spectrum for hyperspectral data

Figure From Menghua Wang, NOAA/NESDIS/STAR

Difficulty of Atmospheric Removal over water

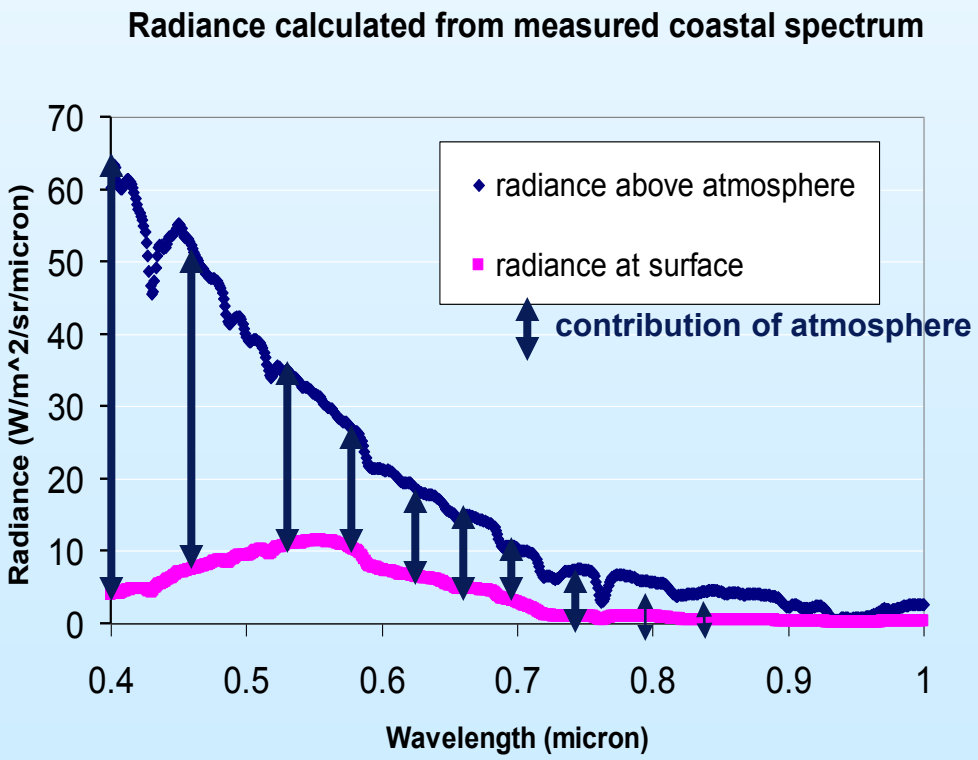

- Atmosphere most of signal
- Atmospheric gasses are well mixed, well understood
- Water is variable
- Aerosols variable in space & time
- Accurate aerosol models and radiative transfer necessary

Tafkaa Atmospheric Correction

- Tafkaa-6-S
  - Based on ATREM (Gao & Davis 1997 PROC SPIE)
  - Uses 6-S atmospheric model
  - User selects aerosol model and optical depth
  - Handles data from all altitudes
  - Changes from ATREM include ability to parse image header file, improve speed, use larger set of aerosol models
- Tafkaa-Tabular
  - Much of the code based on ATREM (Gao & Davis 1997, PROC SPIE)
  - Changes as listed above
  - Uses a large look-up table for the aerosol correction
    - Table created using Zia Ahmed's full vector radiative transfer model
    - Can use dark pixel assumption for open ocean scenes
  - Includes a correction for reflections off of the sea surface
  - Only works for near sea-level data
  - Originally described in (Gao, Montes, Ahmad, & Davis, Applied Optics 2000), modifications in several SPIE proceedings

Tafkaa Atmospheric Correction

The apparent reflectance ρ^*_{obs} at a hyperspectral sensor for a given wavelength is

$$\rho^*_{obs} = \pi L_{obs}/(\mu_o F_o) \qquad (1)$$

where L_{obs} is the radiance of the ocean–atmosphere system measured by the sensor, μ_o is the cosine of the solar zenith angle, and F_o is the extraterrestrial downward solar irradiance at the top of the atmosphere. Then ρ^*_{obs} can be expressed as:

$$\rho^*_{obs} = T_g\,[\rho^*_{atm+sfc} + \rho_w t_d t_u/(1 - s\rho_w)] \qquad (2)$$

where T_g is the total atmospheric gaseous transmittance on the sun-surface–sensor path, $\rho^*_{atm+sfc}$ is the reflectance resulting from scattering by the atmosphere and specular reflection by ocean surface facets, t_d is the downward transmittance (direct + diffuse), t_u is the upward transmittance, s is the spherical albedo that takes into account the reflectance of the atmosphere for isotropic radiance incident at its base, and ρ_w is the water- leaving reflectance. Solving (2) for ρ_w yields

$$\rho_w = \rho^*_{obs}/T_g - \rho^*_{atm+sfc}/[t_d t_u + s\,(\rho^*_{obs}/T_g - \rho^*_{atm+sfc})] \qquad (3)$$

Given L_{obs}, the water-leaving reflectance can be derived according to (1) and (3) provided that the other quantities in the right hand side of (3) can be modeled theoretically.

Tafkaa Look-up Table Generation

We use a modified version of the Ahmad and Fraser code to generate lookup tables for retrieving the required atmospheric parameters. This code includes an atmospheric layering structure that allows for the proper mixing of aerosol particles with atmospheric molecules and the treatment of wind-roughened water surfaces.

The lookup table quantities $\rho^*_{atm+sfc}$, t_d, t_u, and s are functions of wavelength (λ), solar zenith angle (θ_o), view zenith angle (θ), relative azimuth angle ($\varphi - \varphi_o$), aerosol model, optical depth (τ_a), and surface wind speed (W). The values of $\rho^*_{atm+sfc}$. In our lookup table are obtained for a total of 25 aerosol models, 16 MODIS channels, and for the following values of independent variables:

τ_a 0, 0.1, 0.2, 0.3, 0.5, 0.7, 1.0, 1.3, 1.6, and 2.0 at 0.55 μm;

θ_o 1.5 , 12 , 24 , 36 , 48 , 54 , 60 , 66 , and 72 ; 193

θ 0 , 1.5 , 6 , 12 , 18 , 24 , 30 , 36 , 42 , 48 , 54 , 60 , 66 , 72 , 78 , 84 , and 88.5 ;

φ_o 0;

φ 0 , 12 , 24 , 36 , 48 , 60 , 72 , 84 , 90 , 96 , 108 , 120 ,
132 , 144 , 156 , 168 , and 180 ;

W 2, 6, and 10 m/s;

Tafkaa Atmospheric Correction Including Surface Glint Correction for Ocean Scenes

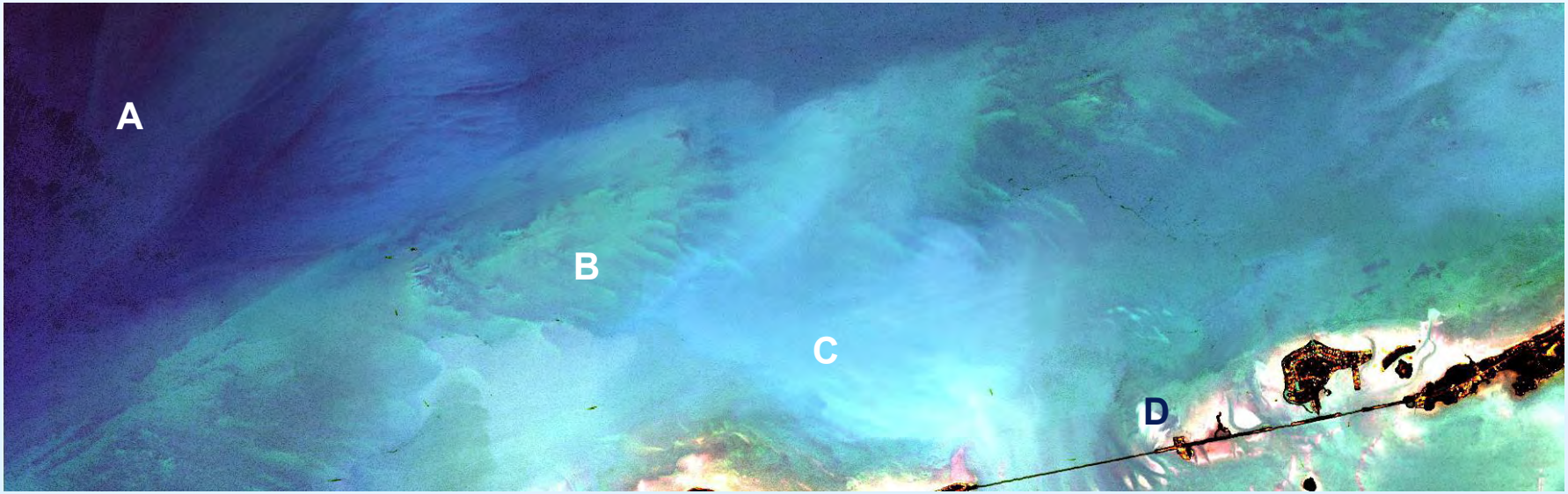

AVIRIS data were atmospherically corrected using the Tafkaa algorithm for ocean scenes. The data are corrected for skylight reflected off the sea surface and then it is assumed that the water leaving radiance is 0 for wavelengths greater than 1.0 micron. (Gao, et al., *Appl. Opt.* 39, 887-896, 2000)

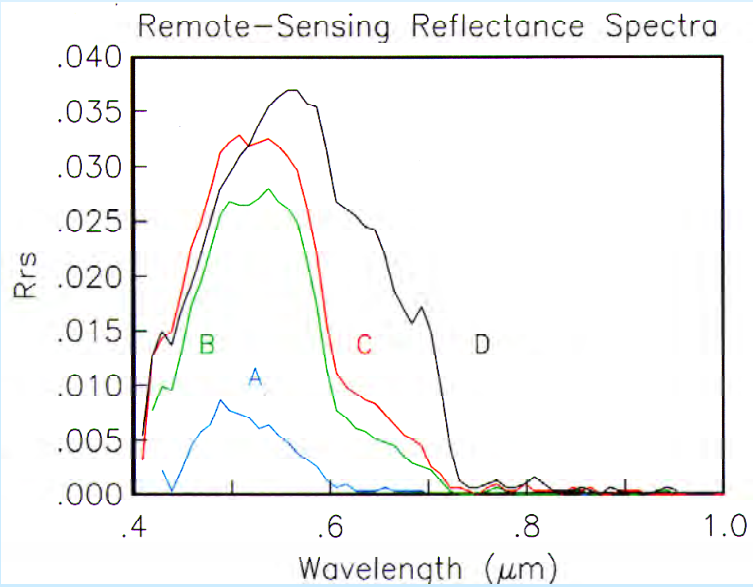

In-water algorithm approaches

Assuming that we have good water leaving radiances these approaches have been used:

A. Regression
B. Neural Networks
C. Look-Up-Table (LUT)
D. Spectral optimization (HOPE)

Regression

(eg., Polcyn 1969, Lyzenga, 1977, 1985; Philpot, 1989)
Developed for use with Landsat data

Example with one spectral band:

$$H \approx \frac{-1}{2K} \ln\left(\frac{L_u - L_{dp}}{\rho E}\right)$$

Key characters:

1. **Need {depth-radiance} pairs to get the empirical coefficients!**
2. **These coefficients are not applicable to other regions.**

Neural Networks (Implicit regression)

$$O = f(I \& W + b)$$

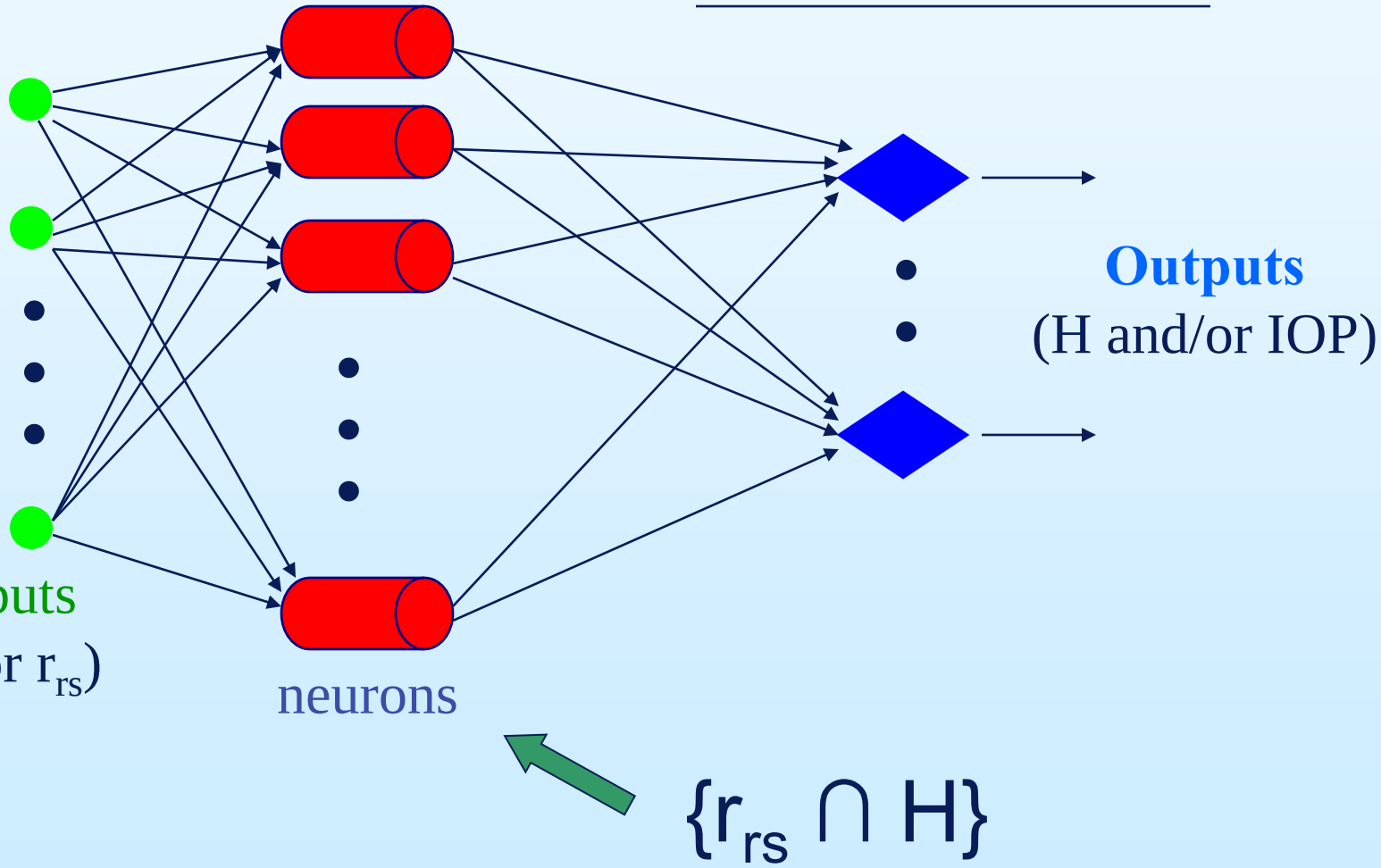

Neural Networks (cont.)

Data Source for Training

a) From measurements (Sandidge and Holyer 1998)

b) From radiative transfer (Lee et al 1998)

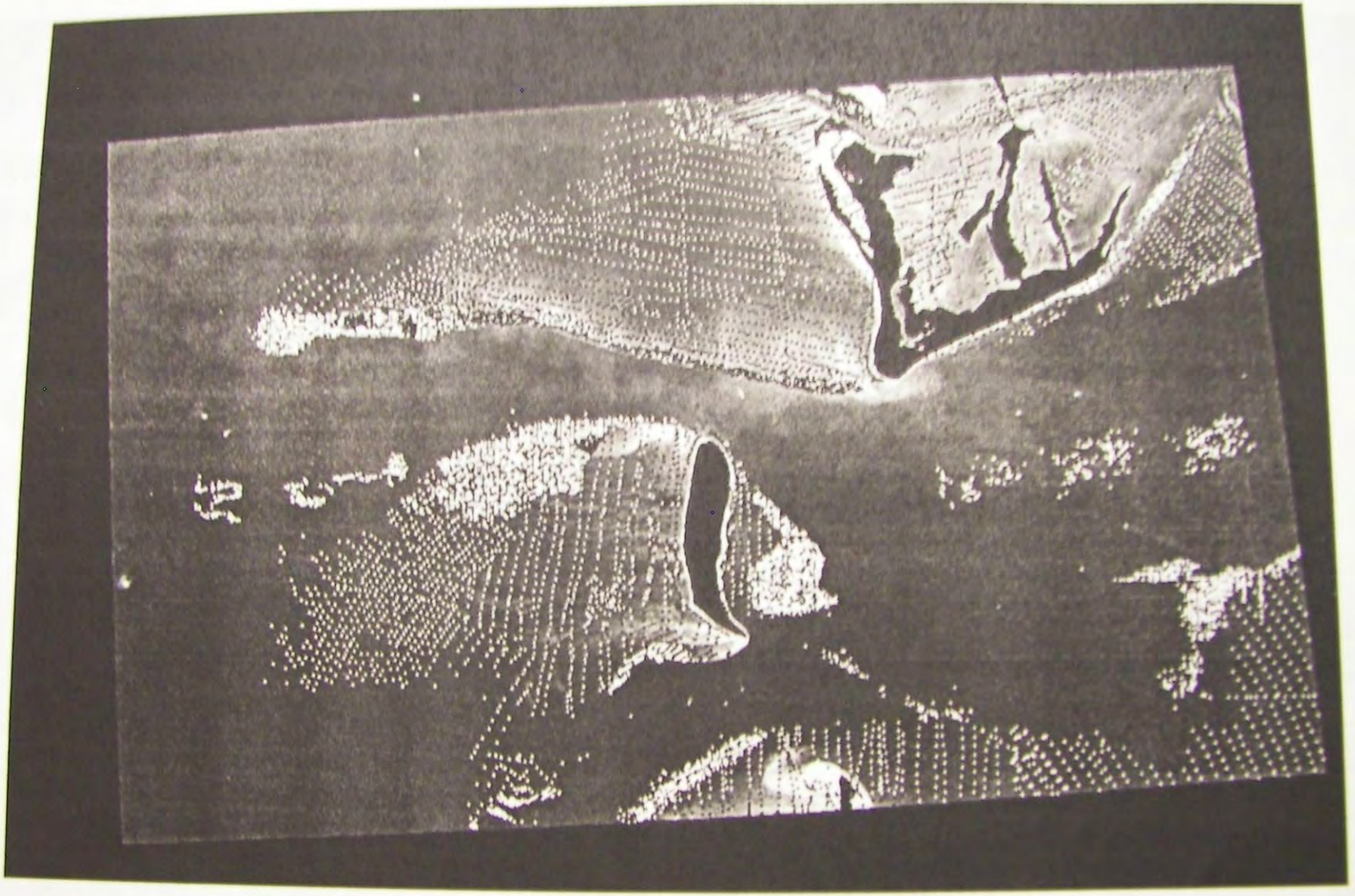

Figure 3. Image of Figure 1 with locations of NOS soundings in the range 0–6 m marked with dots.

(Sandidge and Holyer, 1998)

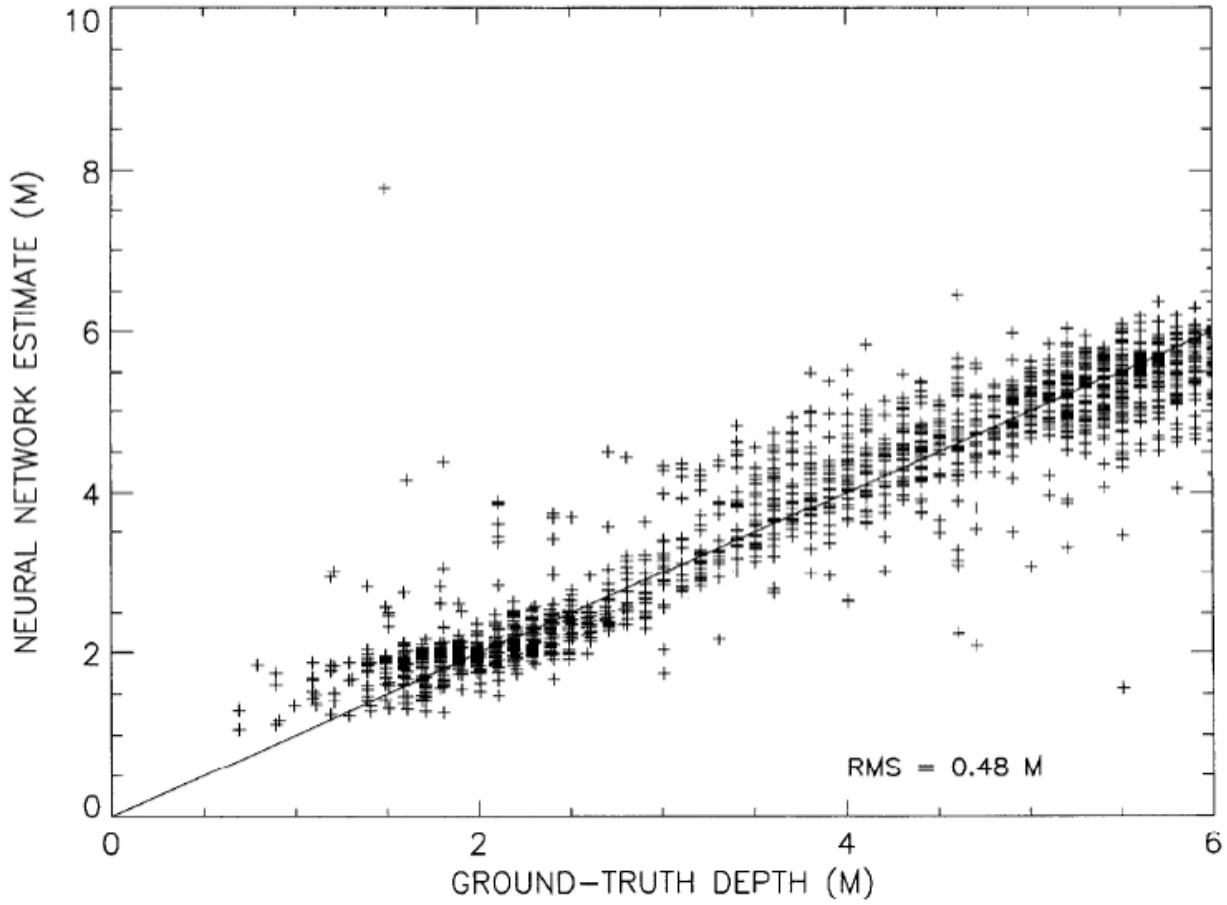

Figure 13. Neural network estimated depths versus ground truth values for the combined test set.

(Sandidge and Holyer, 1998)

The Look-up table approach

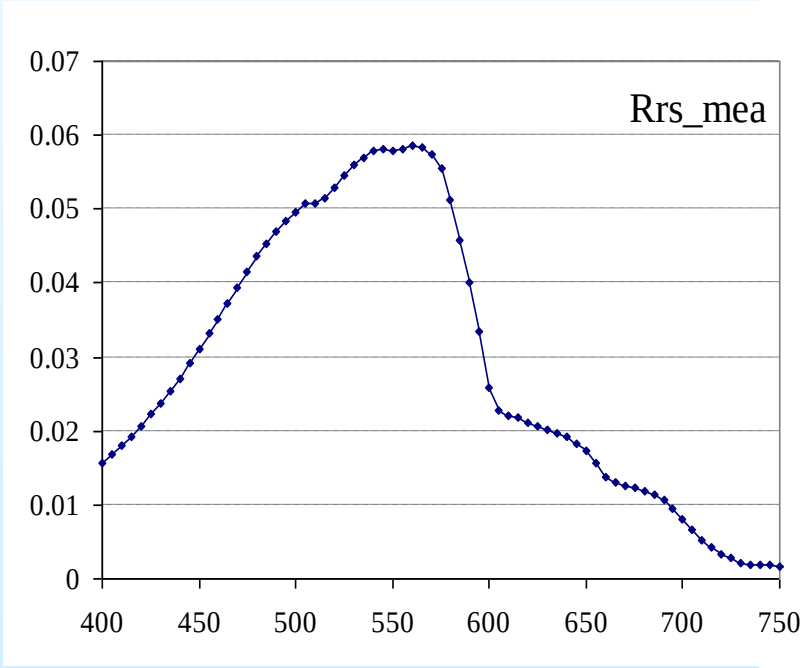

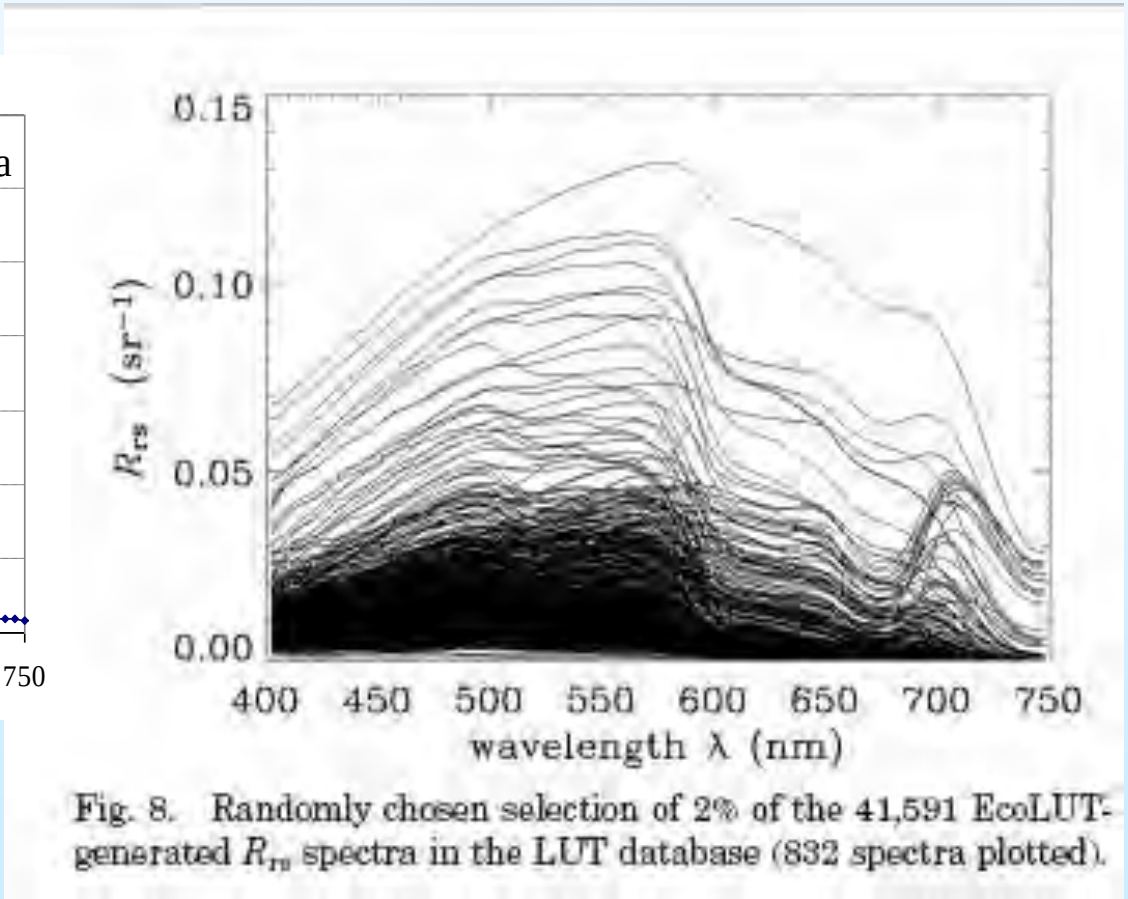

Fig. 8. Randomly chosen selection of 2% of the 41,591 EcoLUT-generated R_{rs} spectra in the LUT database (832 spectra plotted).

(Mobley et al, 2005)

Bathymetry, Bottom Type and Optical Properties using Look-up Tables

Interpretation of hyperspectral remote-sensing imagery via spectrum matching and look-up tables, Mobley, C. D., et al., 2005, Applied Optics, 44(17):3576-3592.

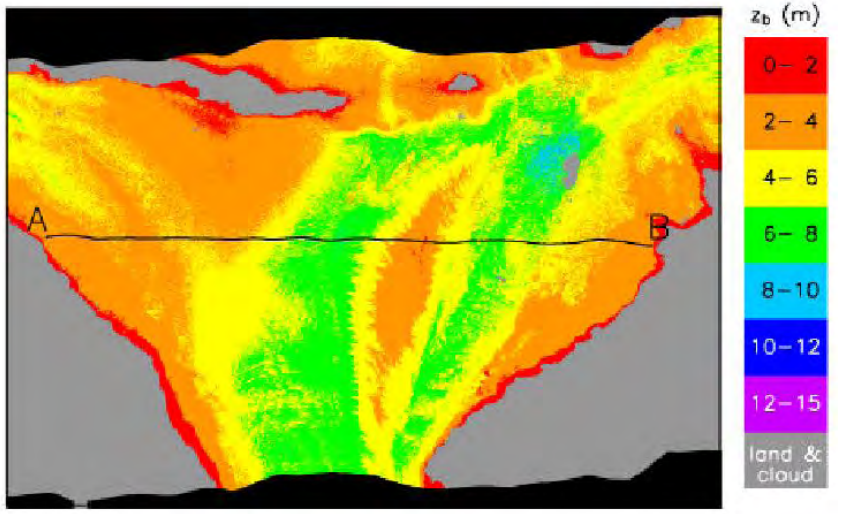

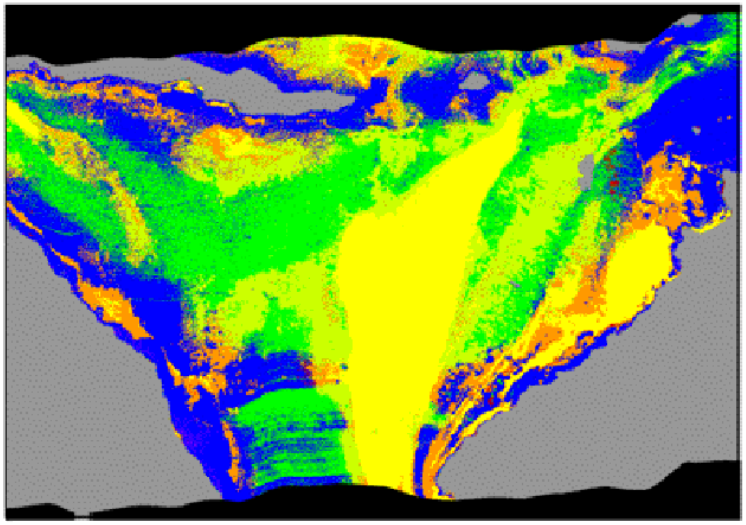

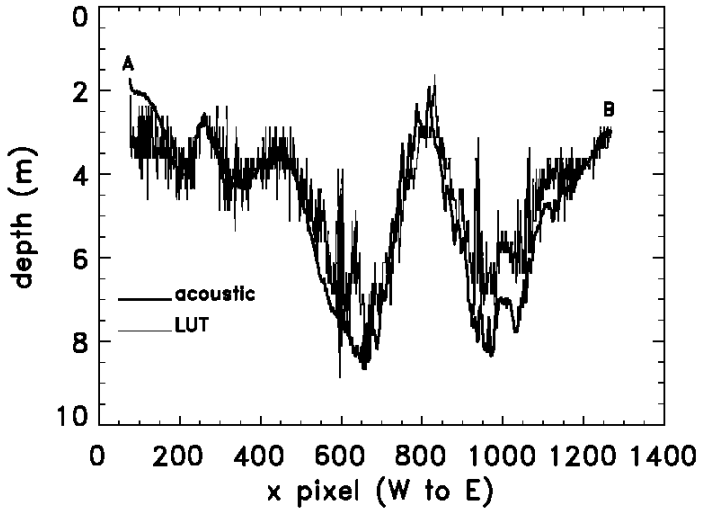

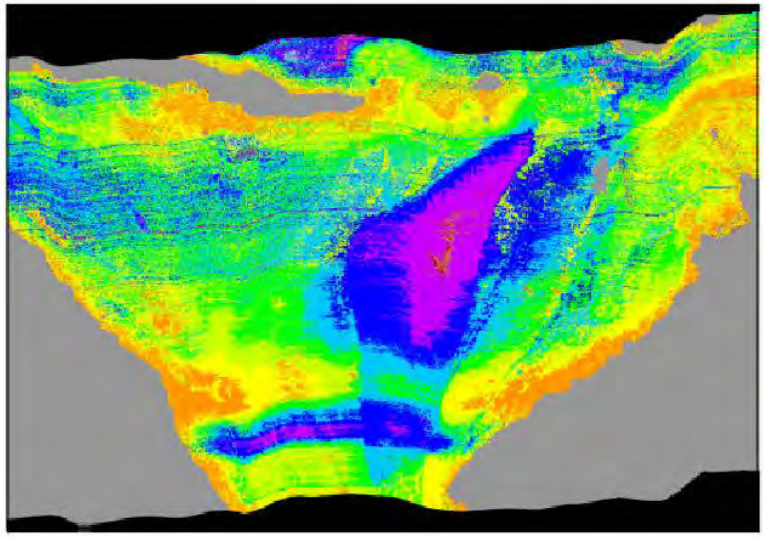

Solving the Shallow Ocean Remote Sensing Problem using Hyperspectral Data

Remote-sensing reflectance (R_{rs}) is a function of properties of the water column and the bottom,

$$R_{rs}(\lambda) = f[a(\lambda), b_b(\lambda), \rho(\lambda), H], \qquad (1)$$

where $a(\lambda)$ is the absorption coefficient, $b_b(\lambda)$ is the backscattering coefficient, $\rho(\lambda)$ is the bottom albedo, H is the bottom depth.

It is desired to *simultaneously* derive bottom depth and albedo and the optical properties of the water column.

Lee et al. (*Appl. Opt.*, 38: 3831-3843, 1999) proposed a new model which can be used with hyperspectral data without the need for ancillary data. They used a semi-analytic model (Lee et al., *Appl. Opt.*, 37: 6329-6338, 1998) for remote sensing reflectance as a function of absorption, scattering, bottom albedo and depth. Then they used a predictor - corrector approach and optimized the result by minimizing an error function.

The Tampa Experiment

- AVIRIS data Was collected over Tampa Bay, FL November 18, 1998 at 1200.
  - AVIRIS was flown on a Twin Otter aircraft at 3810 m giving 4 x 4 m pixels on the ground.
- Remote sensing reflectance, and water properties (chlorophyll *a*, and water absorption coefficients) were measured at a deep-water reference site with uniform water properties that was imaged on the same flight line.
- The result of calibration and atmospheric correction (using MODTRAN 4) of the AVIRIS data was validated by comparing to the reverence site data.
  - The calibration was refined slightly to match the reference data.
- Bathymetry results were compared to ship track measurements and the latest Bathymetric Charts (>20 yrs old).
- A complete description can be found in Lee et al., *J. Geophysical. Research*, 106(C6), 11,639-11,651, 2001.

Hyperspectral Optimization Process Execution (HOPE)

$$r_{rs}(\lambda) = F[a(\lambda), b_b(\lambda), \rho(\lambda), H]$$

- **Basically:**

$$a = a_w + a_\phi + a_g$$

$$b_b = b_{bw} + b_{bp}$$

Values for a_w and b_{bw} are known!
(*Morel 1974, Pope and Fry 1997*)

Unknowns for each $r_{rs}(\lambda)$:

$a_\phi(\lambda)$, $a_g(\lambda)$, $b_{bp}(\lambda)$, $\rho(\lambda)$, and H

HOPE Spectral Models

$$a_\phi(\lambda) = \left(a_0(\lambda) + a_1(\lambda)\ln(\boldsymbol{P})\right)\boldsymbol{P}$$

$$a_g(\lambda) = \boldsymbol{G}e^{-0.015(\lambda - 440)}$$

$$b_{bp}(\lambda) = \boldsymbol{X}\left(\frac{440}{\lambda}\right)^{Y}$$

$$\rho(\lambda) = \boldsymbol{B} * \rho^{+}_{bott}(\lambda)$$

$\boldsymbol{P} = a_\phi(440)$

$\boldsymbol{G} = a_g(440)$

$\boldsymbol{X} = b_{bp}(440)$

$\rho^{+}_{bott}(\lambda) = \rho(\lambda)/\rho(550)$, spectral curvature of bottom reflectance

(Bricaud et al 1981, Smith and Baker 1981, Lee 1994)

Apply model for each wavelength

$$r_{rs}(\lambda) = F[a(\lambda),\ b_b(\lambda),\ \rho(\lambda),\ H]$$

$$\begin{cases} r_{rs}(\lambda_1) = F(a_w(\lambda_1), b_{bw}(\lambda_1), \boldsymbol{P, G, X, B, H}) \\ r_{rs}(\lambda_2) = F(a_w(\lambda_2), b_{bw}(\lambda_2), \boldsymbol{P, G, X, B, H}) \\ \vdots \\ r_{rs}(\lambda_n) = F(a_w(\lambda_n), b_{bw}(\lambda_n), \boldsymbol{P, G, X, B, H}) \end{cases}$$

P: Pigment
G: Yellow substance
X: suspended sediment
B: Bottom
H: Depth

(spectral matching)

$r_{rs}(\lambda)$ from model →← $r_{rs}(\lambda)$ from sensor

Values of: ***P***, ***G***, ***X***, ***B***, and ***H***

(*Lee et al*. 1999, 2001)

HOPE results for Tampa Bay

Tampa Bay comparison to Ship-borne data

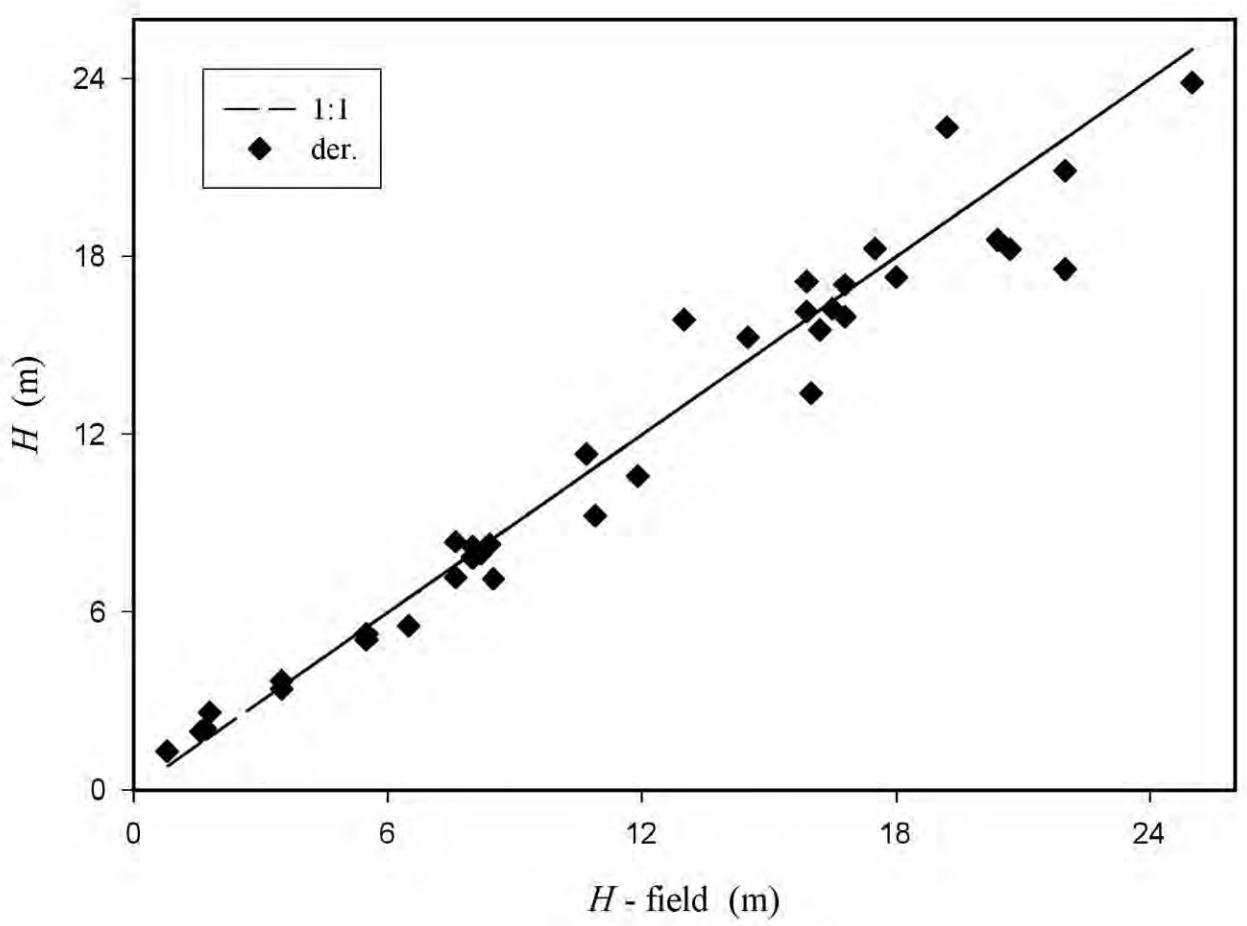

(Lee et al. 1999)

HOPE Results Tampa Bay AVIRIS data

St. Petersburg, FL

Water absorption

St. Petersburg, FL

Bottom depth

(Lee et al. 2001)

Hyperion – Spaceborne Hyperspectral Imagery

Analyzed 6 DATA SETS - HYPERION DATA:

Chesapeake Bay	(19 Feb '02)	
Chesapeake Bay	(6 Sep '02)	
Gulf of Maine	(27 Aug '02)	
Gulf of Mexico	(15 Aug '02)	(Apalachicola Bay, FL)
Bahrain	(27 Aug '02)	
Looe Key, FL	(26 Oct '02)	

ANALYSIS INCLUDES:

Matching With SeaWIFS Imagery

Comparison With In-situ Data From Cruises And Moorings In The Area

Qualitative Identification Of Possible Features

Application Of Remote Sensing Processing Techniques

Quantitative Extraction Of Features And Bathymetry

Identification Of Hyperion Issues

THE NRL TEAM:

Bo-Cai Gao, Marcos Montes, Curt Davis, Bob Arnone and Zhongping Lee (NRLSSC)

Rrs comparison (after Tafkaa)

(Looe Key Hyperion data)

Red : *insitu* Rrs Green: Hyperion Rrs

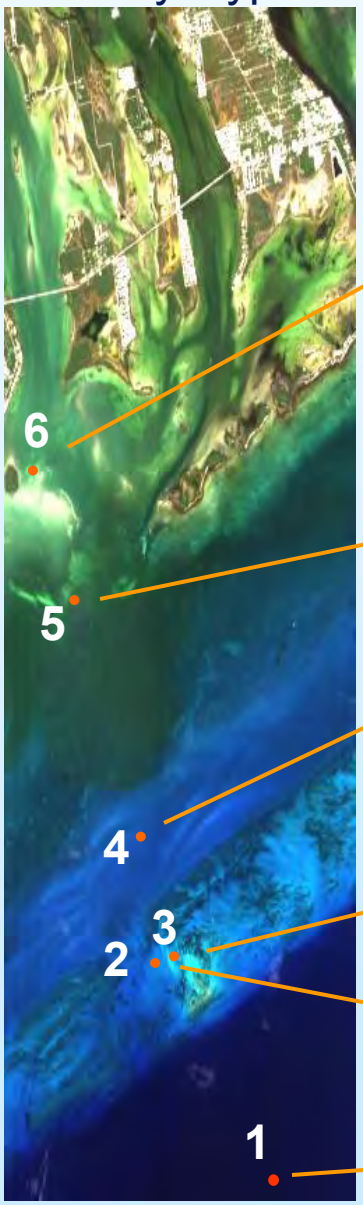

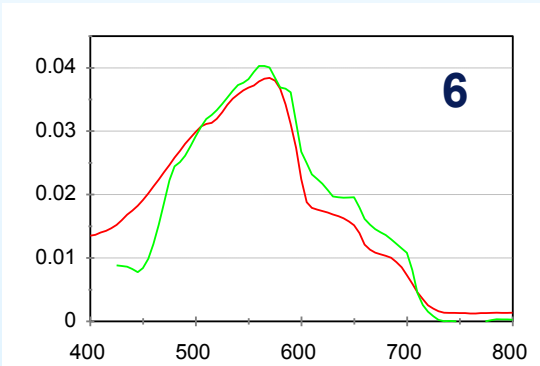

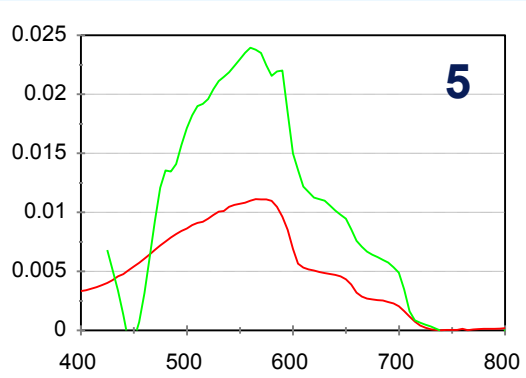

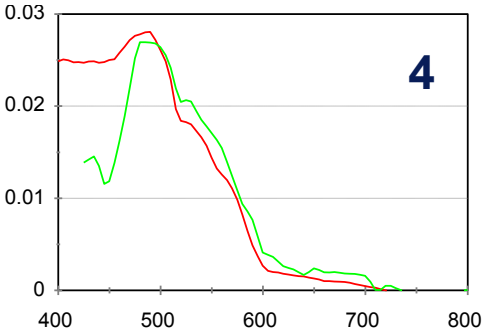

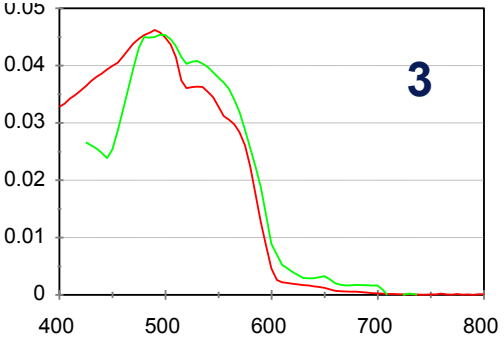

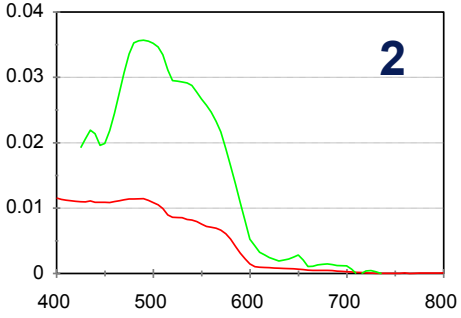

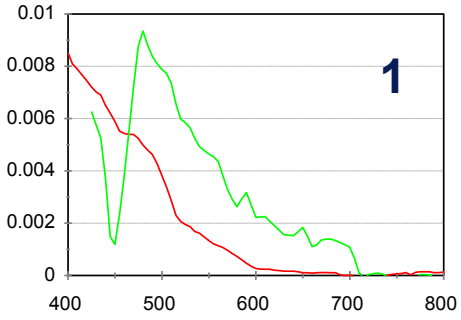

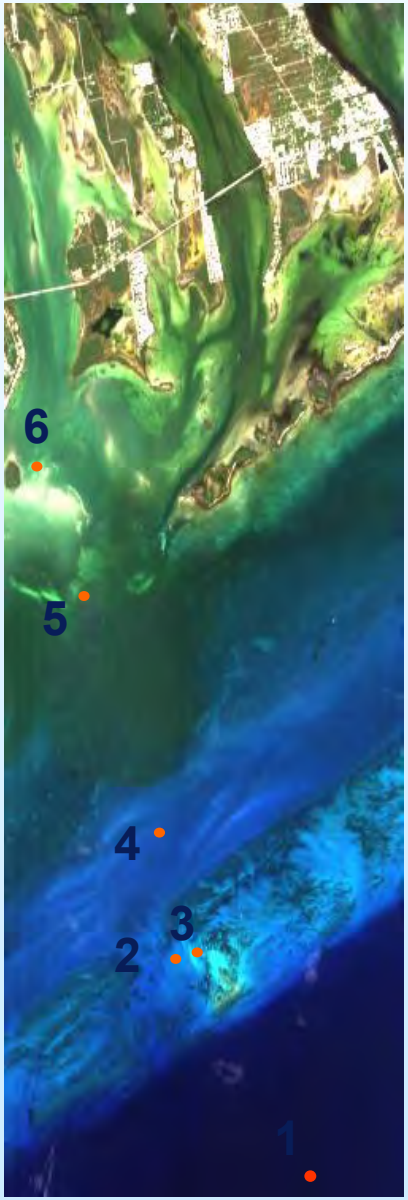

Looe Key Hyperion

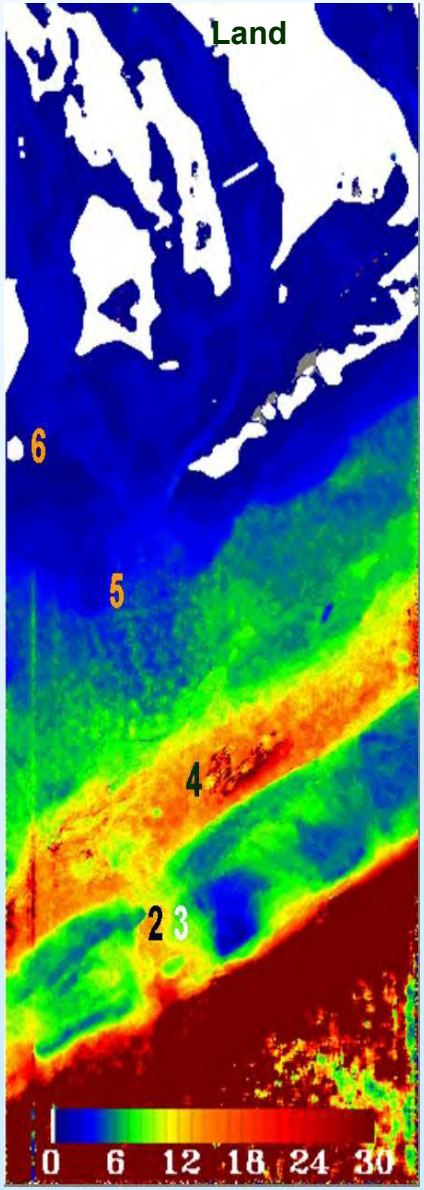

Bottom depth (m)

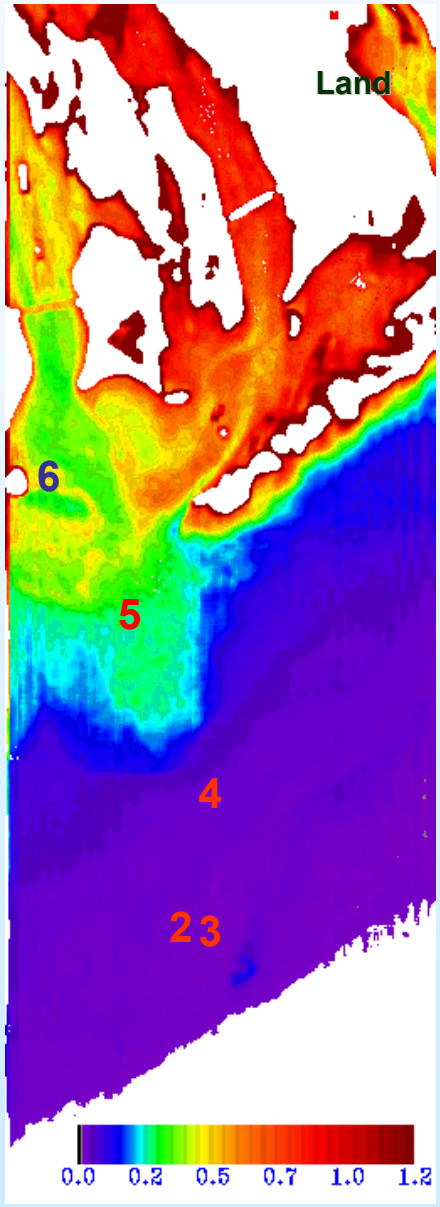

Water absorption at 440 nm (m^{-1})

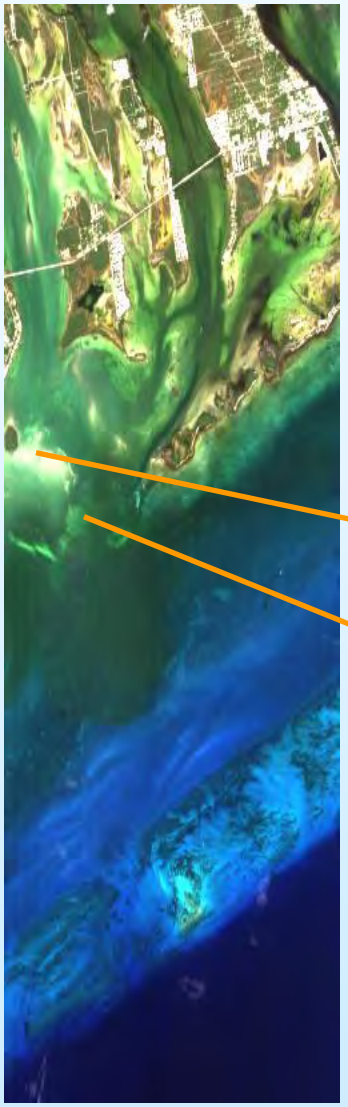

$r_{rs}(\lambda)$ → **HOPE** → (H, IOP, …)

bathymetry

Optical properties

(mea. vs mod. r_{rs})

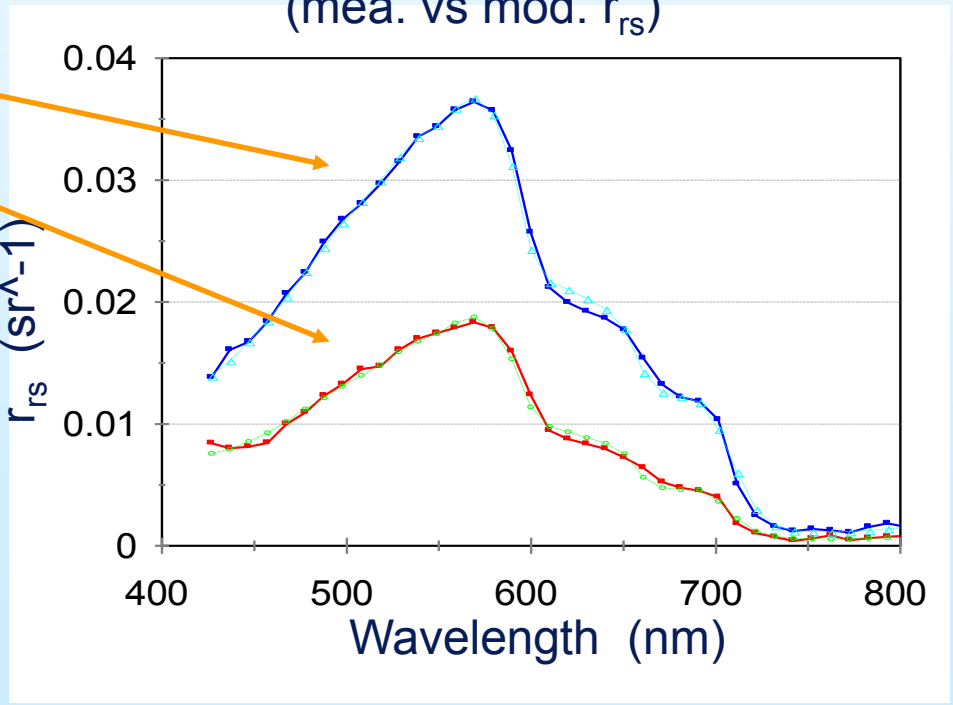

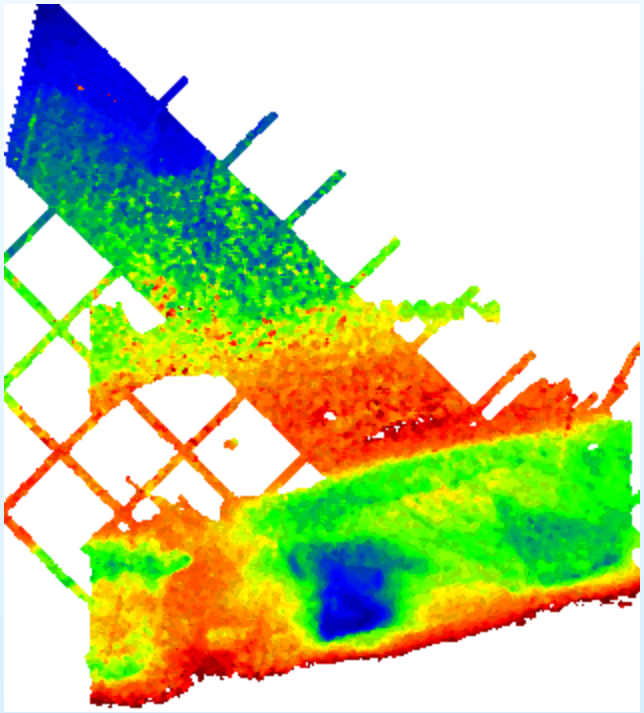

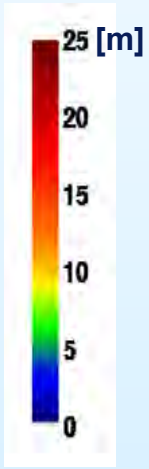

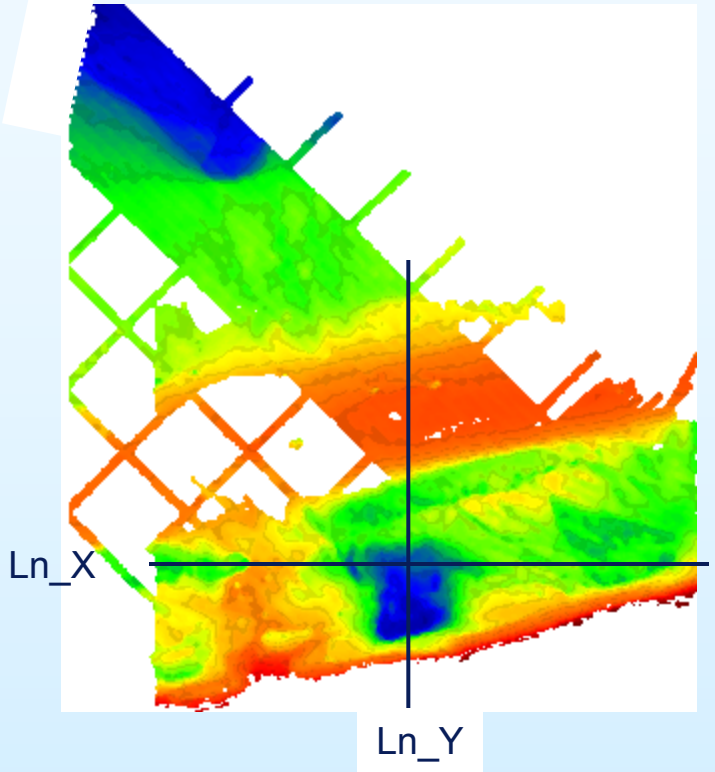

Bathymetry from Hyperion

Bathymetry from LIDAR

HOPE Bathymetry for Hyperion Data

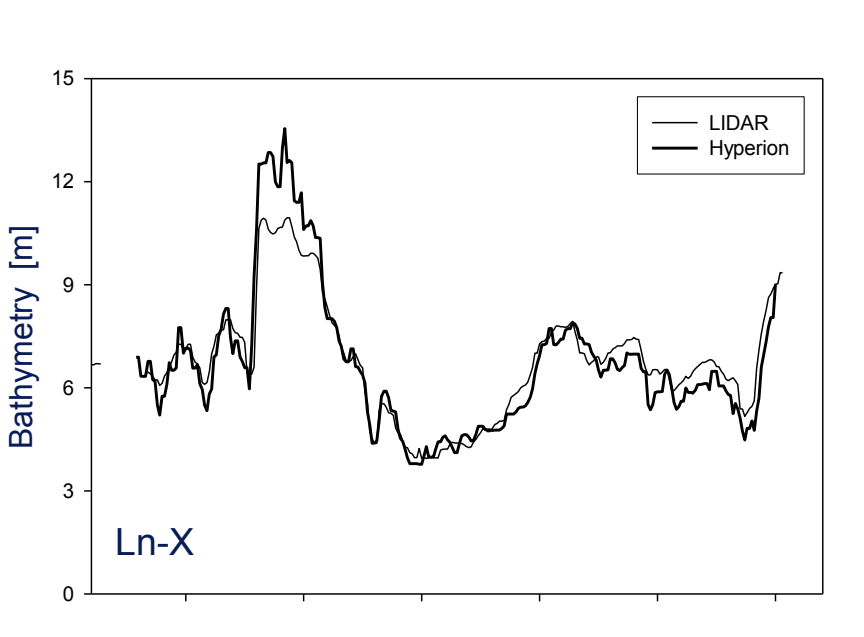

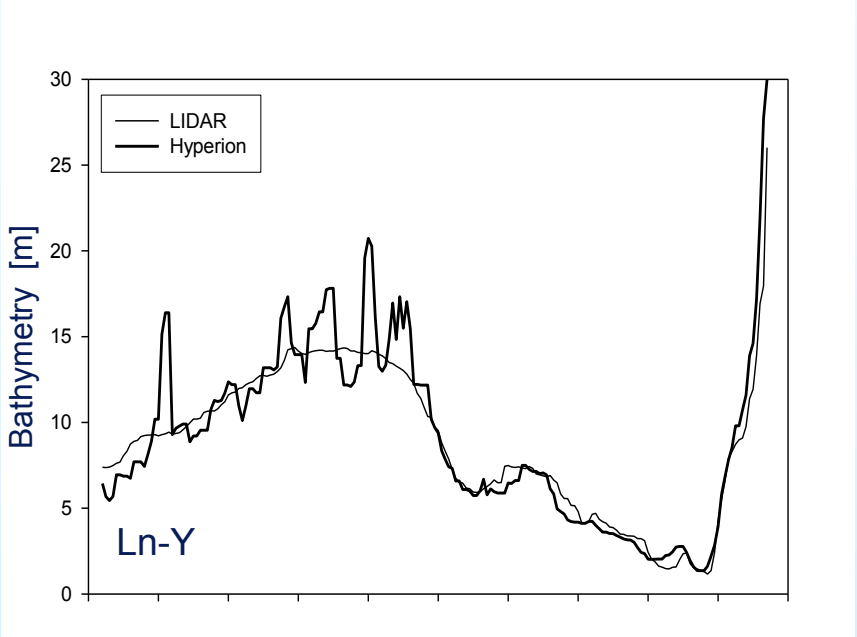

Majority of Data agrees to +/- 10%, with errors apparently associated with a particular bottom type

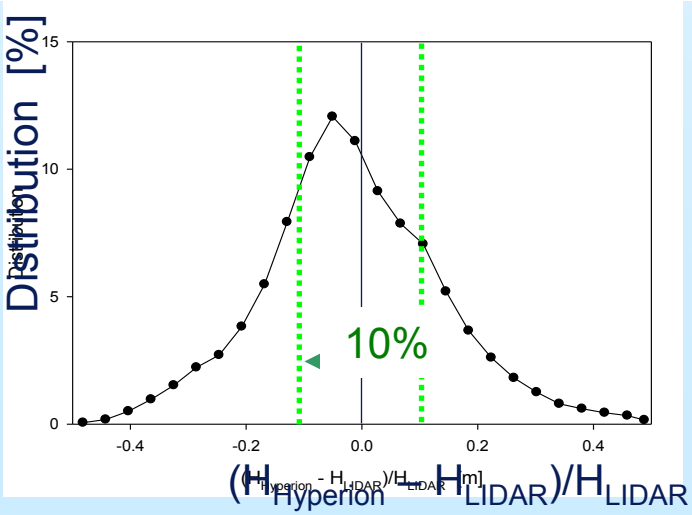

Summary – Hyperion

1) Able to estimate in-water spectra from Hyperion spectra!

- This was better than expected with SNR of 10-50!

2) Applied Optimization methods to water spectra to extract water properties, water depth and bottom reflectance

- Validation is required.

3) Vicarious calibration techniques were required for to overcome SNR and Sun glint (used coincident SeaWIFS data for cross-calibration)

4) Current Hyperion calibration is inadequate for quantitative ocean applications.

5) Atmospheric Correction methods are critical for quantitative analyses

- Several methods used; difficult because of low SNR and calibration issues.

6) The ability to extract ocean products from HYPERION data exceeded expectations indicating the value of having hyperspectral data for the coastal ocean.

Derivative Spectroscopy

What is derivative spectroscopy?

Where are we looking with HICO?
- Lake Erie
- Columbia River
- Yangtze River
- San Francisco Bay

Applications
- Pigment ID
- Product Indicator Maps

[Preliminary work by Nick Tufillaro]

Derivative Spectroscopy

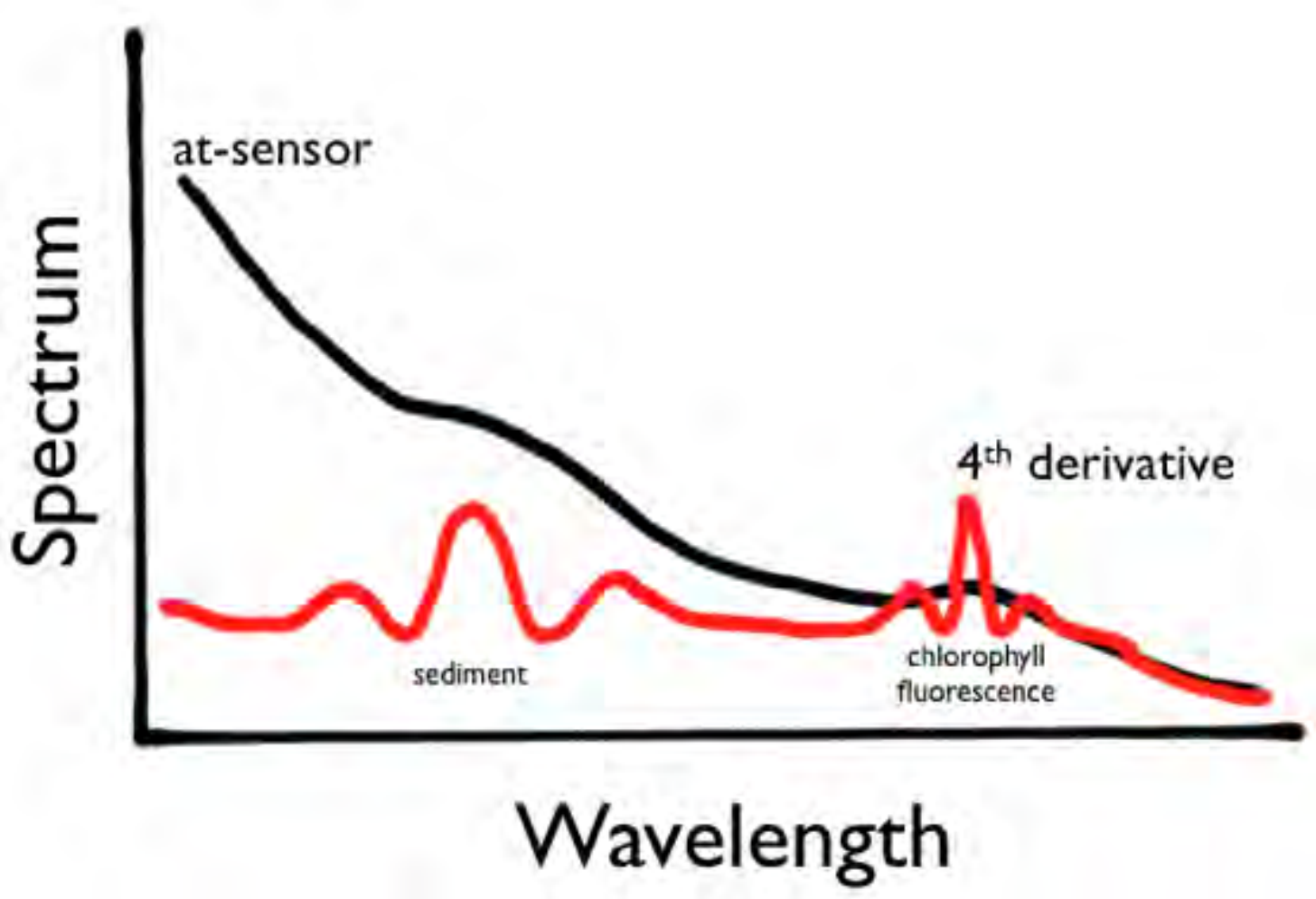

Savitzky-Golay Filter (Polynomial Smoothing)

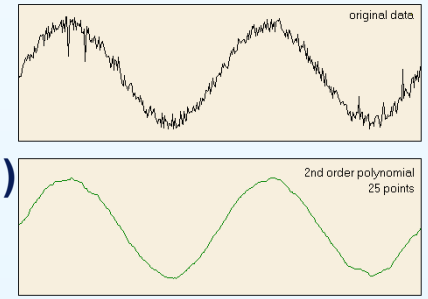

4th Derivative Spectra Computed From HICO

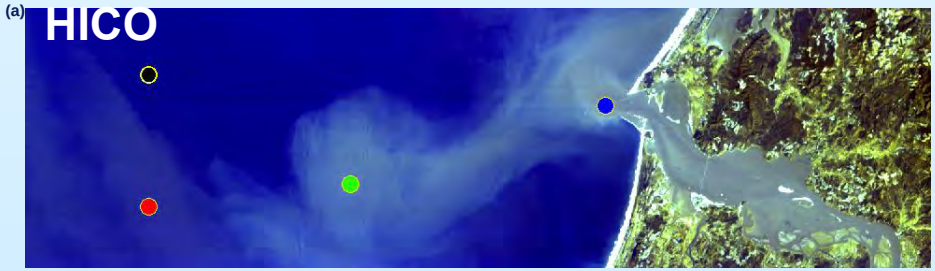

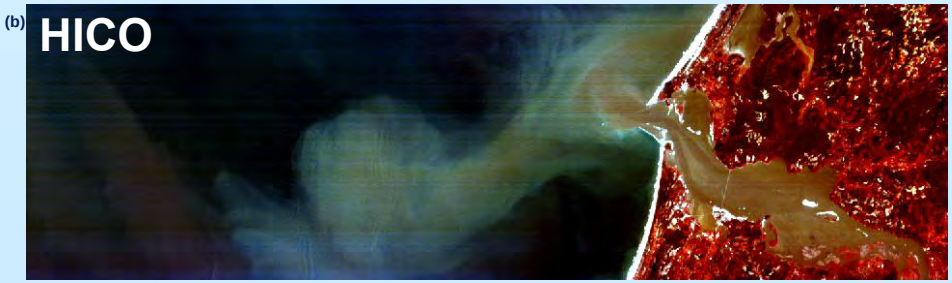

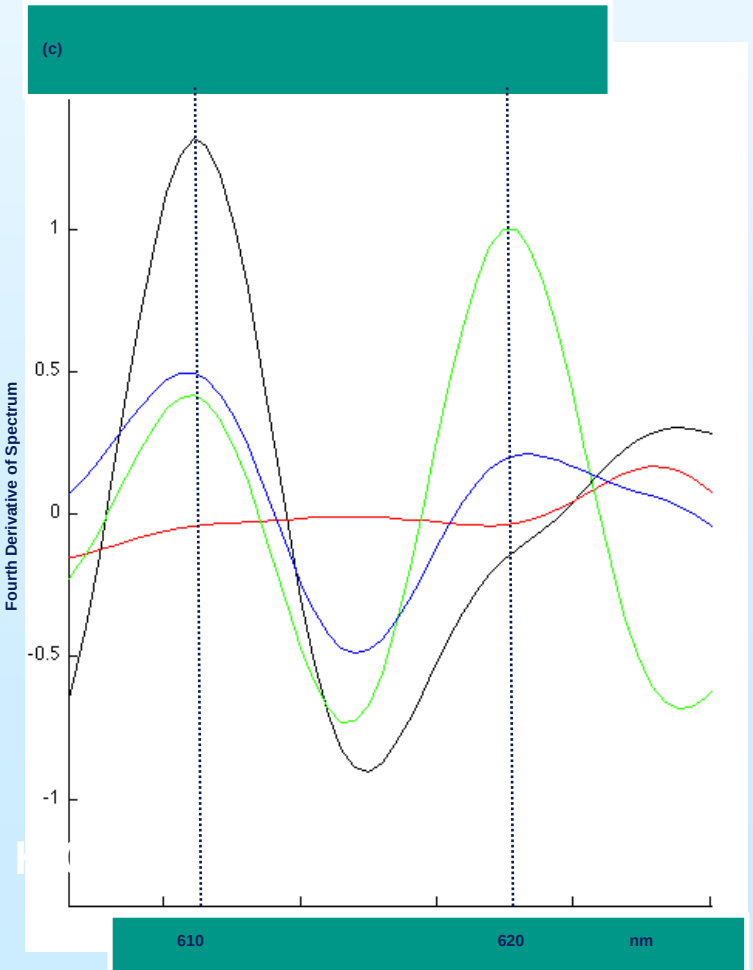

Relating derivatives to spectral features

Biology

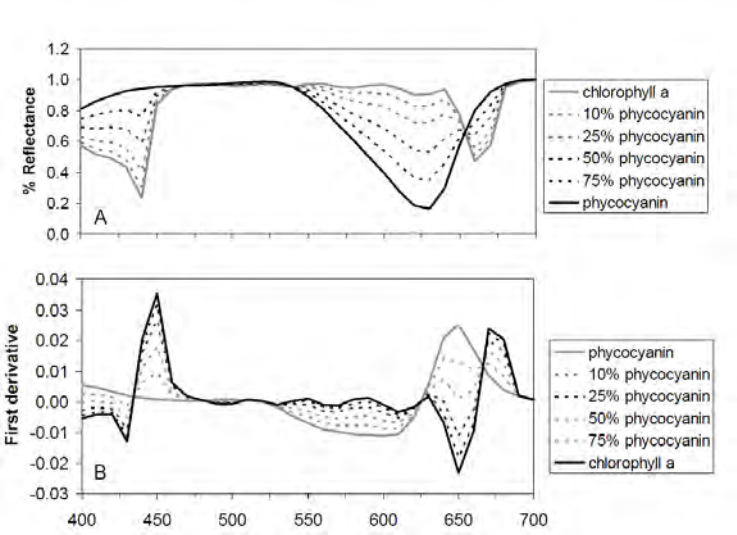

Minerals

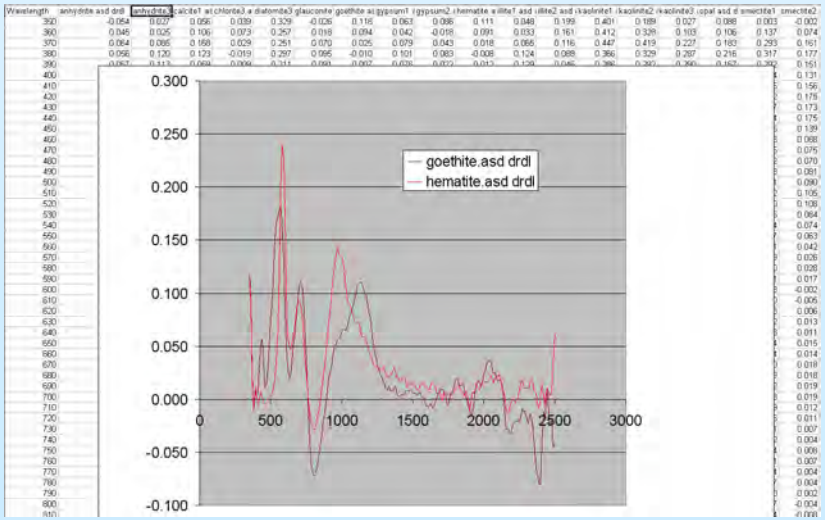

PCA to develop signatures

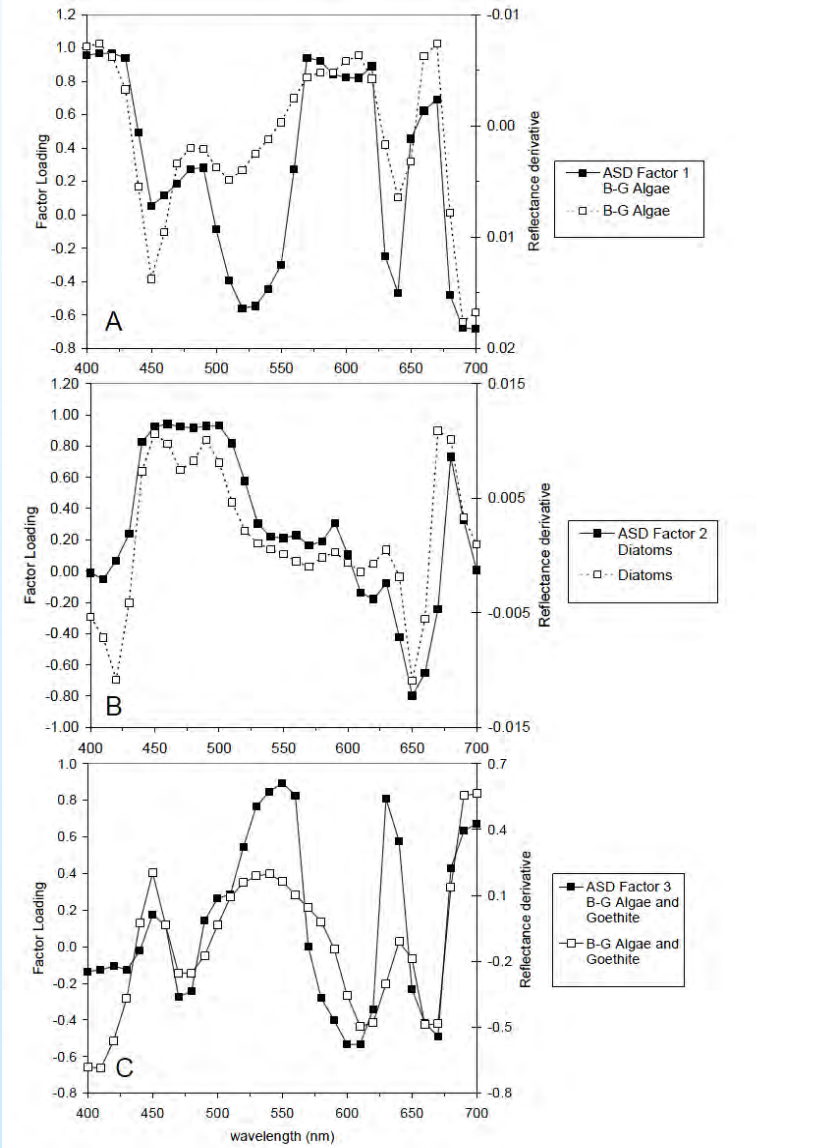

Data from Joe Oritz, Ohio State University

Microcystis bloom in Lake Erie

HICO Image of a massive *Microcystis* bloom in western Lake Erie, September 3, 2011 as confirmed by spectral analysis.

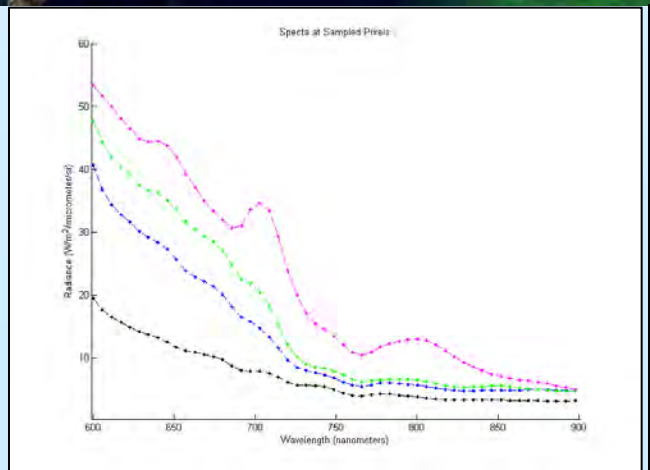

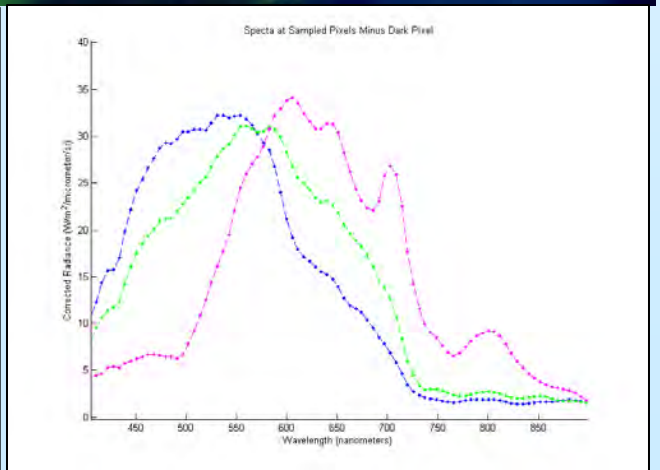

HICO L2 Spectra for Western Lake Erie 2011 09 03

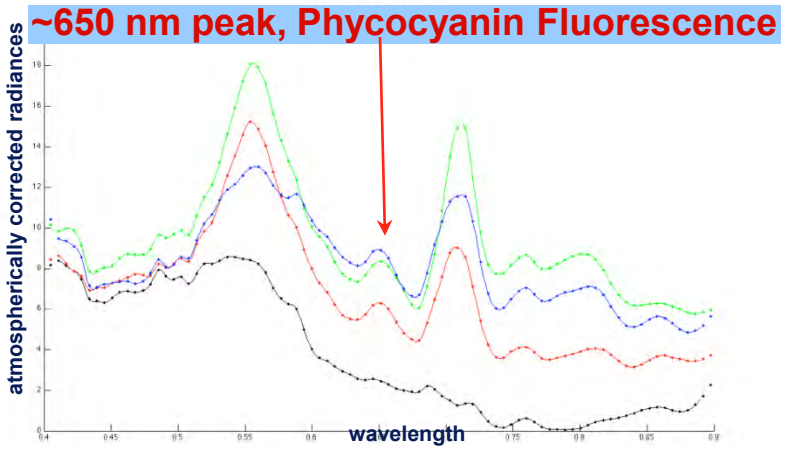

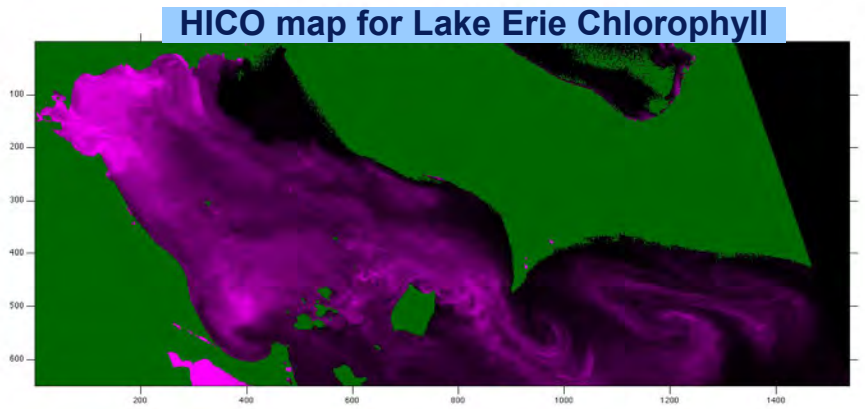

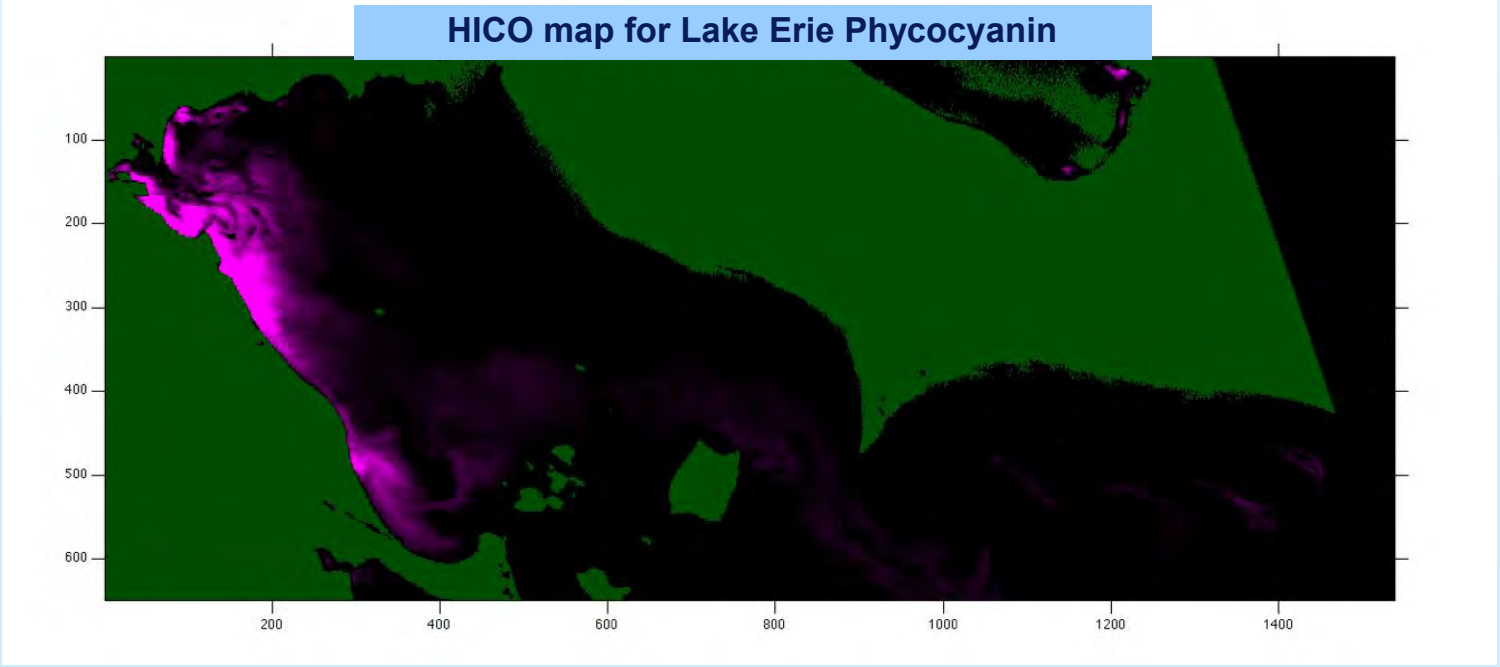

GOCI image of the Waters around Korea

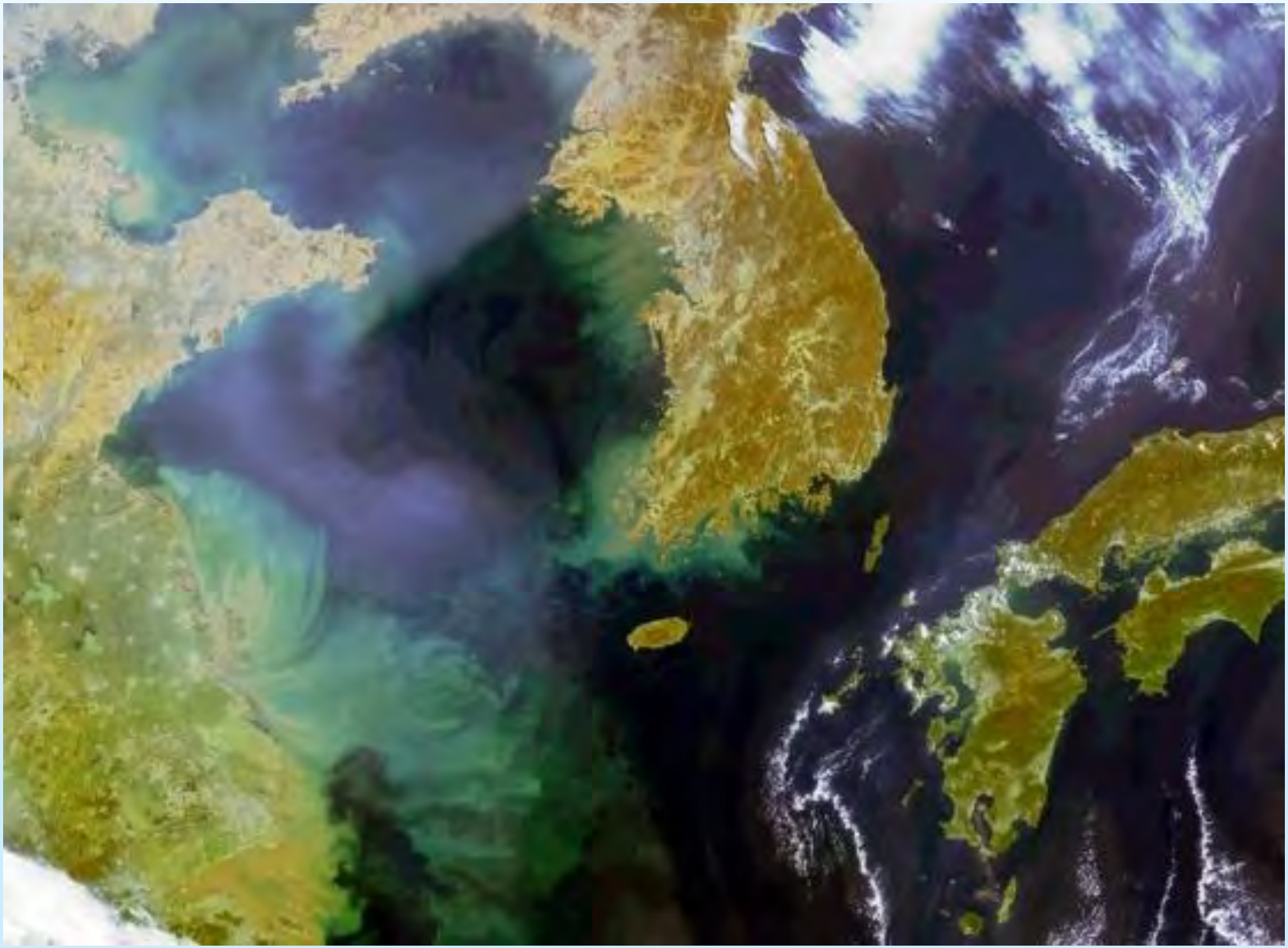

Coincident HICO image of the Yangtze River

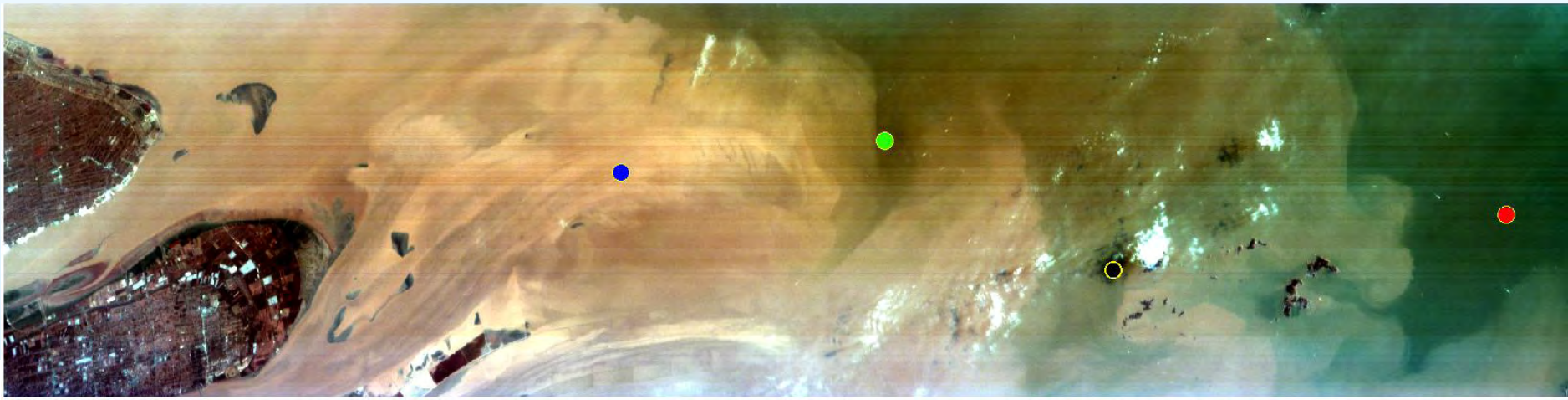

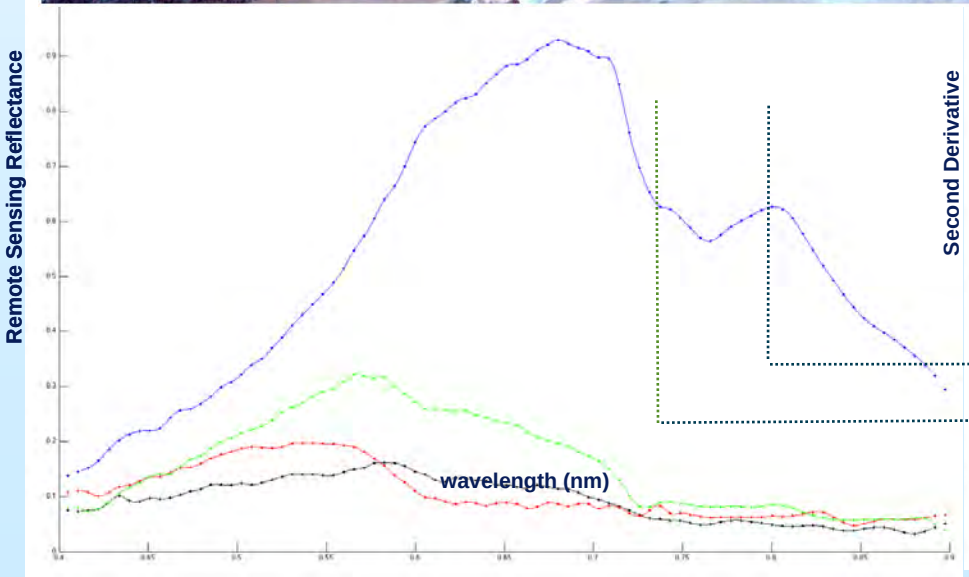

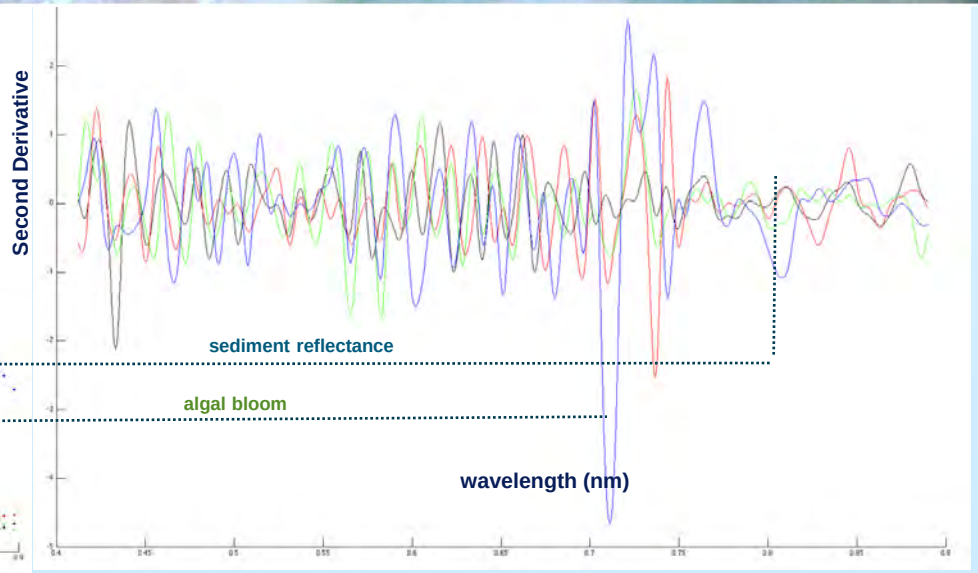

HICO image of San Francisco Bay and adjacent waters

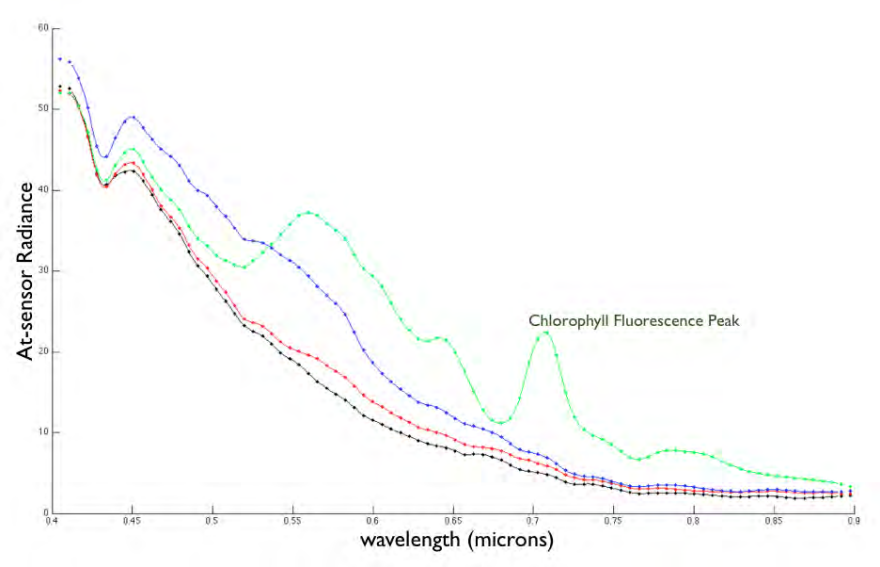

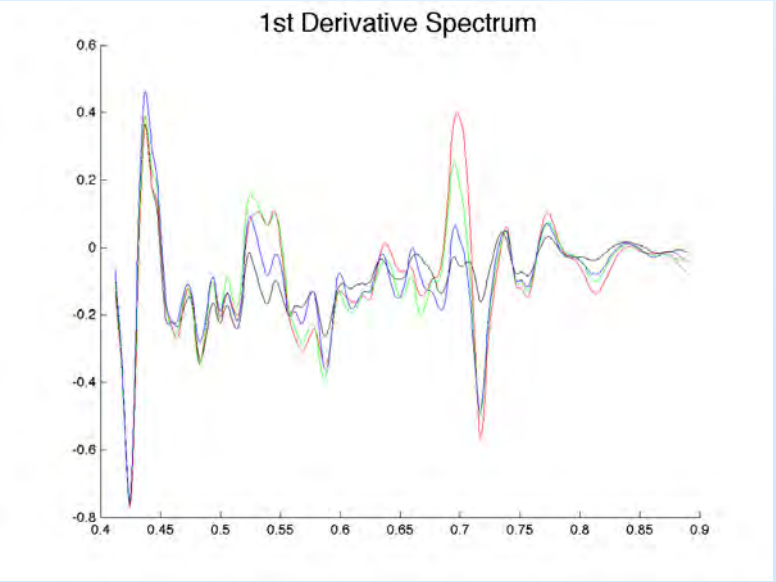

Spectral Difference in 'Embedding Space'

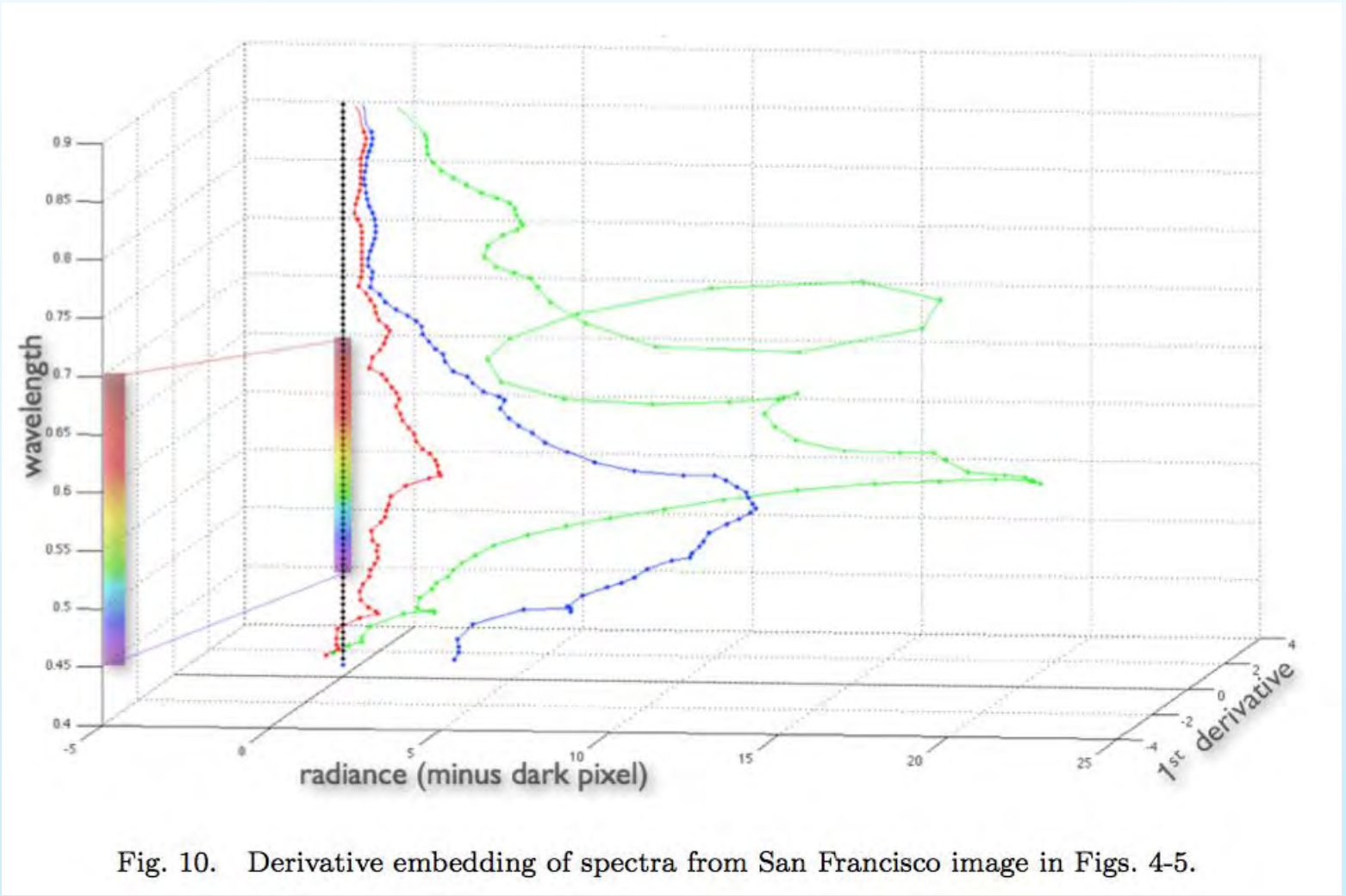

Fig. 10. Derivative embedding of spectra from San Francisco image in Figs. 4-5.

Euclidean norm between between two spectral samples,

$$d(\lambda_n) = \sqrt{(L_b - L_a)^2 + \ldots + (L_b^{n'} - L_a^{n'})^2}$$

The shape of ocean color, chapter in the book
"From Laser Dynamics to Topology of Chaos,"
R. Gilmore and C. Letellier eds., World Scientific, 2012.

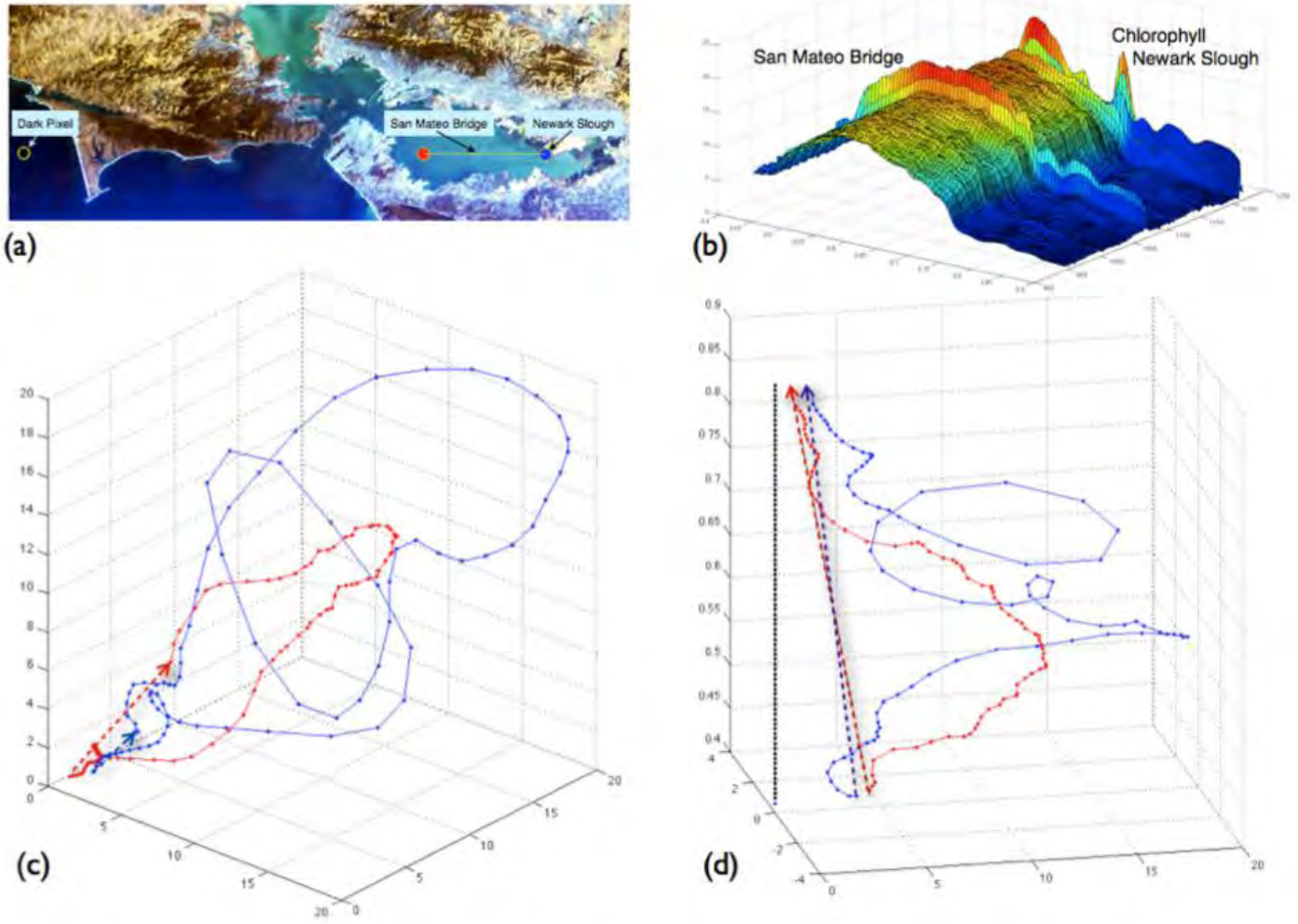

Fig. 11. Embedded spectra for the HICO scene (a) of the San Francisco Bay (28 September 2011). The sample points are indicated by red and blue dots in (a), and the line of spectra between the two end points is shown in (b). The sample points pass over the San Mateo bridge which is easy to see in (b), and the Newark Slough in the South Bay with high chlorophyll levels. A delay embedding of the spectrum for the sample points in (a) is shown in (c). The embedding curve can be 'closed' by attaching the end points which is indicated by a dotted line with an arrow. The associated braid spectra (d) can also be closed by attaching endpoints. The linking between the spectra is $\mathcal{L} = 1$ in both embeddings (c) and (d).

torsion, writhe, linking, and all that ...

Calling this axis curve $\mathbf{x}(s)$, the tangent vector to the axis curve is,

$$\hat{\mathbf{T}}(s) = \frac{d\mathbf{x}}{d\mathbf{s}}.$$

Define $\hat{\mathbf{V}}(s)$ to be the unit normal to $\hat{\mathbf{T}}(s)$, the normal vector points in the direction $\mathbf{y}(s) = \mathbf{x}(s) + \epsilon\hat{\mathbf{V}}(t)$. The tube inherits a local coordinate system from the axis curve, namely (s, ϕ), where the secondary curve $\mathbf{y}(s)$ has coordinates $(s, 0)$. A choice of $\mathbf{y}$ fixes the coordinate system and is called a 'framing'.[18] If we set $\hat{\mathbf{W}} = \hat{\mathbf{T}} + \hat{\mathbf{V}}$ then the tube surface is traced out by

$$\mathbf{y}(s, \phi) = \mathbf{x}(s) + \epsilon(\cos\phi\hat{\mathbf{V}}(s) + \sin\phi\hat{\mathbf{W}}(s)).$$

The 'Frenet frame' describes the local geometry of the axis curve. Define the 'curvature,' κ,

$$\kappa = |\frac{d\hat{\mathbf{T}}(s)}{ds}|.$$

The 'normal' and 'binormal' vectors are ($\kappa \neq 0$),

$$\hat{\mathbf{N}} = \frac{1}{\kappa}\frac{d\hat{\mathbf{T}}(s)}{ds}, \qquad \hat{\mathbf{B}} = \hat{\mathbf{T}} \times \hat{\mathbf{N}}.$$

Taken together, the vectors $\{\hat{\mathbf{T}}, \hat{\mathbf{N}}, \hat{\mathbf{B}}\}$ form a orthonormal right handed basis with 'torsion,' τ, described by the Frenet-Serret equations,

$$\frac{d\hat{\mathbf{T}}(s)}{ds} = \kappa\hat{\mathbf{T}}, \qquad \frac{d\hat{\mathbf{N}}(s)}{ds} = \tau\hat{\mathbf{B}} - \kappa\hat{\mathbf{T}} \qquad \frac{d\hat{\mathbf{B}}(s)}{ds} = -\tau\hat{\mathbf{T}}.$$

For the framing choose $\hat{\mathbf{V}} = \hat{\mathbf{N}}$.

The Gauss linking number is typically defined in terms of a double integral.[14] Here we use the the fact the spectral braid is open and parameterized by λ to compute the linking number in terms of a sum of single integral.[15] Consider the rotation, or winding, about the vertical direction, z, along the wavelength axis in Fig. 10. The linking number can be expressed as a 'winding angle' of curves as we trace them out in the z (wavelength) direction. Consider two spectral braids $\mathbf{x}_i$ and $\mathbf{y}_i$, and their difference vector at a height z, $\mathbf{r}_{ij}(z) = \mathbf{x}_j(z) - \mathbf{x}_i(z)$. The rotation rate of $\mathbf{r}_{ij}$ is given by,

$$\frac{d\Theta_{ij}}{dz} = \frac{\hat{\mathbf{z}} \cdot \mathbf{r}_{ij} \times \mathbf{r}'_{ij}(z)}{|\mathbf{r}_{ij}(z)|^2},$$

and the net winding number is

$$\Delta\Theta_{ij} = \int_{z_1}^{z_2} \frac{d\Theta_{ij}}{dz}.$$

Divide the curve into pieces separated by the turning points $dz/ds = 0$, indexed by z_i to z_j and define

$$\sigma_i(z) = \begin{cases} -1, & z \in (z_i, z_{i+1}) \quad \& \quad dz/ds < 0 \\ +1, & z \in (z_i, z_{i+1}) \quad \& \quad dz/ds > 0 \\ 0, & z \notin (z_i, z_{i+1}). \end{cases}$$

Then the linking number between the two curves can be shown to be:[15]

$$\mathcal{L}_k = \sum_{i=1}^{n}\sum_{j=1}^{m} \frac{\sigma_1\sigma_j}{2\pi}\Delta\Theta_{ij}.$$

For our product indicators, it will turn out that the net winding number between two curves, $\tilde{\Lambda} = \int_{z_1}^{z_2} \frac{d\tilde{\Lambda}}{dz} dz$ is initially more useful than the linking.

The Calŭgăreanu theorem states that the linking is equal to the twist plus the writhe,

$$\mathcal{L}_k = \mathcal{T}_w + \mathcal{W}_r.$$

application: edge detection

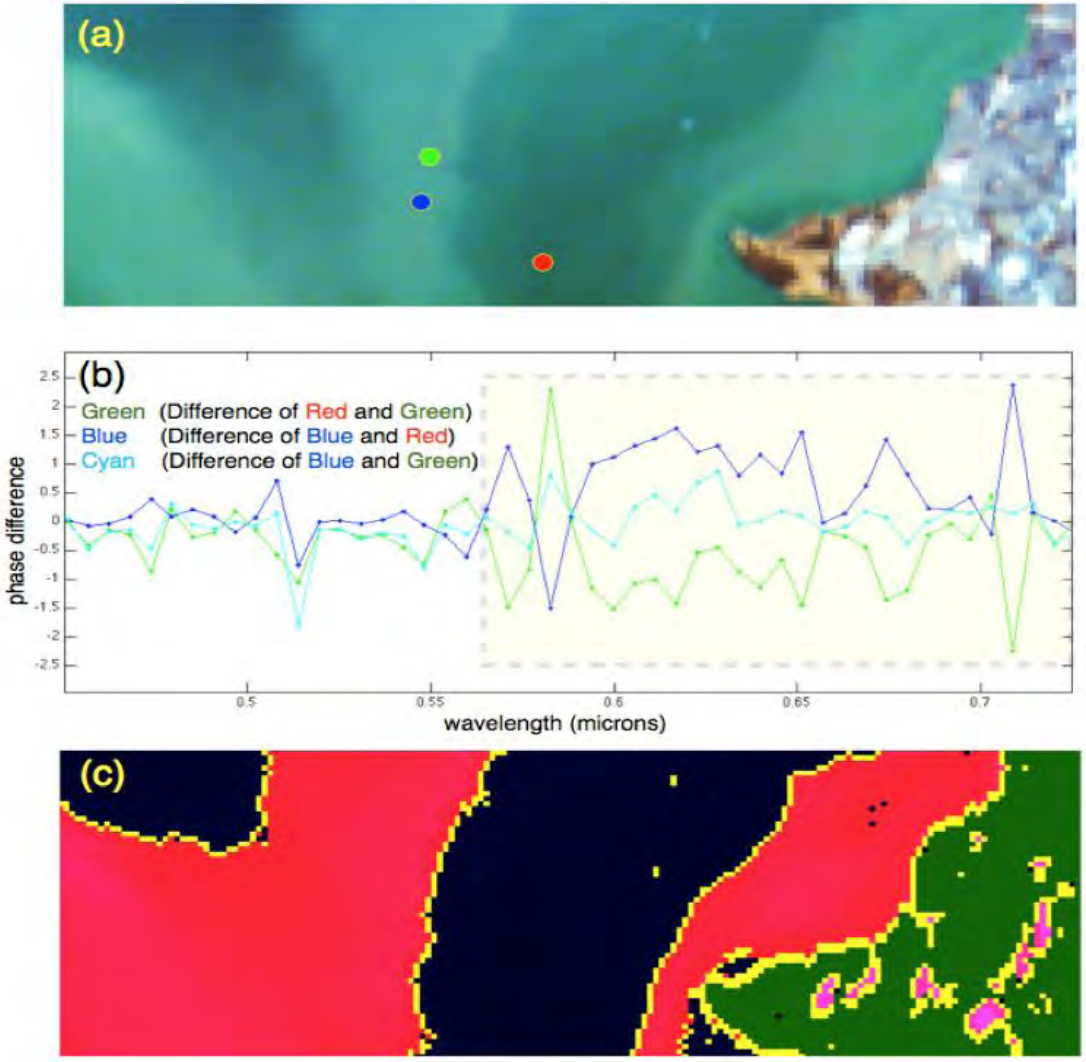

Fig. 12. HICO image of San Pablo Bay off of Pinole Point Park (a) 28 September 2011. (b) The phase difference computed from the 'winding number' of the spectra indicated bt the colored dots in (a). (c) Edge detection is computed from phase difference between $0.575\ nm < \lambda < 0.75\ nm$. The edge detection identifies the San Pablo Strait.

application: product indicators

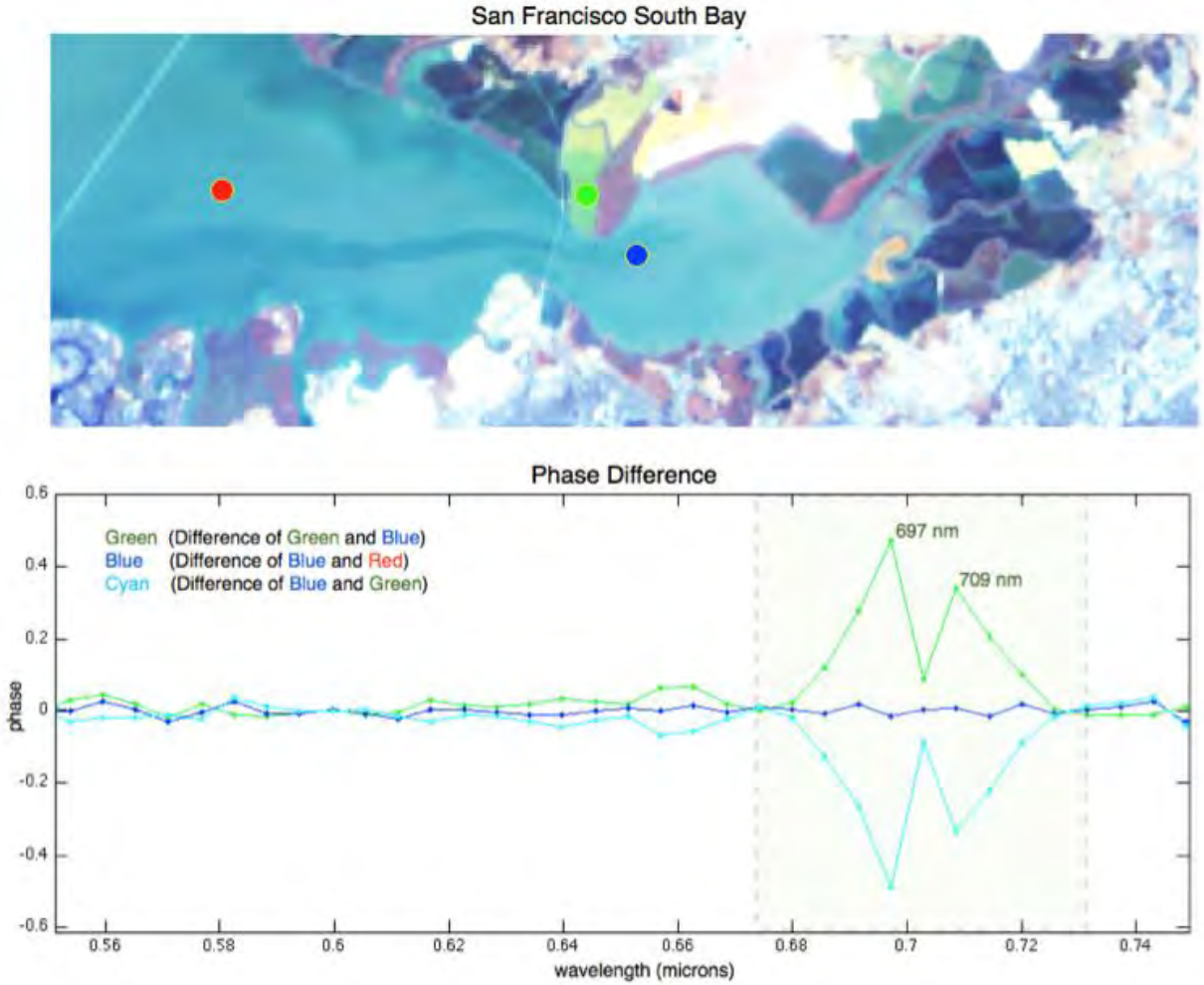

Fig. 13. HICO image of the South San Francisco Bay 28 September 2011 (top). The green dot indicates spectra from the Newark Slough which is an algae mat. The lower plot shows the phase difference between the spectra from the Newark Slough and the surrounding bay water. The extremas at 0.697 and 0.709 can be used to create an indicator function for the algae mat.

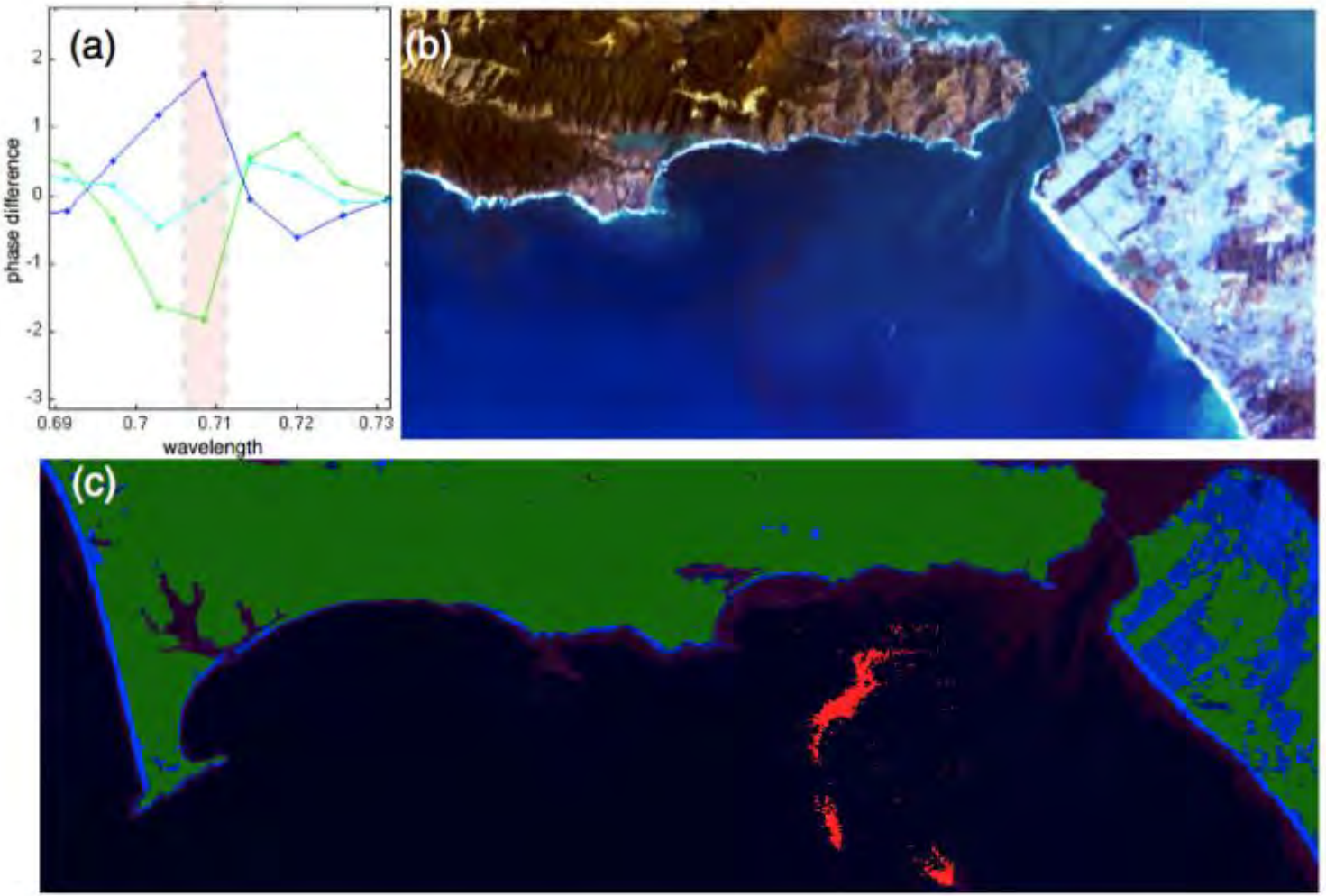

Fig. 14. (a) The phase difference function for spectra at the mouth of the San Francisco Bay showing that the 709 nm HICO channel can be used to indicated chlorophyl rich water. (b) HICO image of mouth of San Francisco Bay, 28 September 2011. (c) Indicator function for high chlorophyll levels which appear to show a high concentration of chlorophyll at the interface of bay water and sea water.

How we got started - A Tribute to Alex Goetz

- Alex Goetz and co-authors defined and demonstrated imaging spectrometry and hyperspectral imaging in a 1985 article in Science.
- Ocean imaging spectrometry started by Ken Carder and Curt Davis proposing to use AVIRIS data for coastal applications in 1987.
- The High Resolution Imaging Spectrometer (HIRIS) was selected in 1989 as part of the NASA EOS program with Alex Goetz as the team leader.
  - Curt Davis and Ken Carder selected as ocean team members; Curt subsequently became the JPL Program Scientist
  - Though the launch would be a decade away under Alex's leadership the team developed:
    - ATREM (forerunner to Tafkaa and current land algorithms)
    - SIPS the forerunner of ENVI (Industry standard for processing HSI data
    - Alex saw the need for compact, well-calibrated field spectrometers and founded ASD (field spectrometers for product validation).
    - A host of applications for geology, ecology and oceanography were initially developed for HIRIS.
  - HIRIS was cancelled during a round of major cost cutting for the EOS program but the legacy of HIRIS lives on.
- We are still waiting for a HIRIS quality imaging spectrometer in Space.

Conclusions and the Way Ahead

- Ocean imaging spectrometry started by Ken Carder and Curt Davis 25 years ago using AVIRIS data for coastal applications in 1987.
- We now have good airborne sensors including commercial and very small sensors for UAVs.
- We have achieved good calibration, atmospheric correction and product validation for a variety of coastal environments.
  - No automated, accurate atmospheric correction
- There are several methods for solving for optical properties, bottom type and bathymetry
  - Look-up tables
  - Semi-analytical models
  - But these methods have problems with inaccurate data and they do not directly address the inherent non-linearity of the data
- Great improvement is possible by
  - Integrated approach to calibration, atmospheric correction and in-water products
- We are still waiting for a quality imaging spectrometer in Space.
  - Impressive results from Hyperion given low SNR and calibration issues
  - HICO provides good quality 100 m data but 3X SNR better
  - EnMAP in 2015, SNR? PACE 2019, ACE, GEO-CAPE 2020+ Others?

Additional References

- Davis, C. O., J. T. O. Kirk, J. S. Parslow and S. Sathyendranath, 2000, Measurement Requirements for Case 2 Waters, in Remote Sensing of Ocean Colour in Coastal, and Other Optically-Complex Waters, S. Sathyendranath ed., Int. Ocean-Colour Coordinating Group, Dartmouth, NS, Canada, Report #3: 77-92.
- Davis, C. O., J. Bowles, R. A. leathers, D. Korwan, T. V. Downes, W. A. Snyder, W. J. Rhea, W. Chen, J. Fisher, W. P. Bissett and R. A. Reisse, 2002, "Ocean PHILLS hyperspectral imager: design, characterization, and calibration", *Optics Express*, 10(4): 210-221.
- Gao, B.-C., M. J. Montes, Z. Ahmad, and C. O. Davis, 2000, "An atmospheric correction algorithm for hyperspectral remote sensing of ocean color from space", *Appl. Opt*. 39(6): 887-896.
- Lee, Z. P., K. L. Carder, C. D. Mobley, R. G. Steward and J. S. Patch, "Hyperspectral remote sensing for shallow waters: 1. A semi-analytical model", *Appl. Opt.*, 37: 6329-6338, 1998.
- Lee, Z. P., K. L. Carder, C. D. Mobley, R. G. Steward and J. S. Patch. (1999) Hyperspectral remote sensing for shallow waters: 2. Deriving bottom depths and water properties by optimization. *Applied Optics*, *38*, 3831-3843, 1999.
- Lee, Z. P., K. L. Carder, R. F. Chen, and T. G. Peacock, "Properties of the water column and bottom derived from Airborne Visible Infrared Imaging Spectrometer (AVIRIS) data", *J. Geophys. Research*, 106(C6), 11,639-11,651, 2001.
- Mobley, C. D., L. K. Sundman, C. O. Davis, T. V. Downes, R. A. Leathers, M. J. Montes and J. H. Bowles, W. P. Bissett, D. D. R. Kohler, R. P. Reid, E. M. Louchard and A. Gleason, 2005, "Interpretation of hyperspectral remote-sensing imagery via spectrum matching and look-up tables", *Appl. Opt.*, 44(17): 3576-3592.
- Sandidge, J. C. and R. J. Holyer, "Coastal bathymetry from hyperspectral observations of water radiance", *Remote Sensing of Environment*, 65: 341-352, 1998.

GEO-CAPE Geostationary Ocean Color Imager

Why Geostationary given MODIS, VIIRS, etc?

- Tides, diel winds (such as the land/sea breeze), river runoff, upwelling and storm winds drive coastal currents that can reach several knots. Furthermore, currents driven by diurnal and semi-diurnal tides reverse approximately every 6 hours.
- daily sampling at the same time cannot resolve tides, diurnal winds, etc.
- GEO-CAPE could resolve tides from a geostationary platform and will provide the management and science community with a unique capability to observe the dynamic coastal ocean environment.
- GEO-CAPE could provide higher spatial resolution (500 m vs. 1000 m)
- GEO-CAPE could be hyperspectral to measure solar stimulated fluorescence, suspended sediments, CDOM and improved atmospheric correction.

These improvements are critical for the analyses of coastal waters.

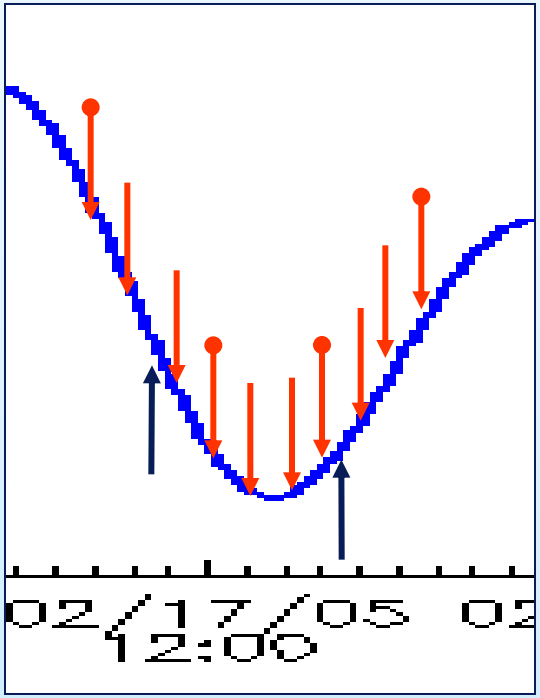

Example tidal cycle from Charleston, OR. Black arrows MODIS sampling, red arrows GEO-CAPE sampling.

The Coastal Ocean Applications and Science Team (COAST)

- The Coastal Ocean Applications and Science Team (COAST) was created in August 2004 to support NOAA to develop coastal ocean applications for a geostationary ocean color imager HES-CW:
  - Mark Abbott, Dean of the College of Oceanic and Atmospheric Sciences (COAS) at Oregon State University is the COAST team leader,
  - COAST activities are managed through the Cooperative Institute for Oceanographic Satellite Studies (CIOSS) a part of COAS, Ted Strub, Director
  - Curtiss Davis, Senior Research Professor at COAS, is the Executive Director of COAST.
  - Initial activity to evaluate HES-CW requirements and suggest improvements
  - Conducted Monterey Bay experiment during first year of funding.
- The Hyperspectral Environmental Suite including the Coastal Waters instrument (HES-CW) was dropped from GOES-R in November 2006.
- Here we report initial results from the Monterey Bay experiment
  - Use the airborne hyperspectral data to assess spatial, temporal and spectral sampling requirements for a Coastal Waters Imaging System (CWIS).

Risk Reduction Activities: Principal Roles of Co-Investigators

- **Curtiss Davis**, program management, calibration, atmospheric correction
- **Mark Abbott**, COAST Team Leader
- **Ricardo Letelier**, phytoplankton productivity and chlorophyll fluorescence, data management
- **Peter Strutton**, coastal carbon cycle, Harmful Algal Blooms (HABs)
- **Ted Strub**, CIOSS Director, coastal dynamics, links to IOOS

COAST Participants:

- **Bob Arnone, NRL**, optical products, calibration, atmospheric correction, data management
- **Paul Bissett, FERI**, optical products, data management
- **Heidi Dierssen, U. Conn.**, benthic productivity
- **Raphael Kudela, UCSC**, HABs, IOOS
- **Steve Lohrenz, USM**, suspended sediments, HABs
- **Oscar Schofield, Rutgers U.**, product validation, IOOS, coastal models
- **Heidi Sosik, WHOI**, productivity and optics
- **Ken Voss, U. Miami**, calibration, atmospheric correction, optics

NOAA/STAR Menghua Wang, atmospheric correction

NOAA/STAR Mike Ondrusek, calibration, MOBY

NOAA/NOS Rick Stumpf, HABs

NOAA/NMFS Cara Wilson, Ecosystem Management of Fisheries

Monterey Bay September 3-16, 2006 Experiment Plan

- Goal to collect a data set that include all the key attributes of CWIS data:
  - Spectral coverage (.4 – 1.0 μm)
  - High signal-to-noise ratio (>300:1 prefer 900:1, for ocean radiances)
  - High spatial resolution (<100 m, bin to 300 m)
  - Hourly or better revisit
- Monterey Bay has long-term physical, biological and optical monitoring
  - Links to data at http://www.cencoos.org
- COAST conducted Intensive effort for 2 weeks supplementing the standard data sets to assure that all essential parameters are measured
- Aircraft overflights for at least three clear days and one partially cloudy day (to evaluate cloud clearing) during the two week period.
  - High altitude to include 90% or more of the atmosphere
  - 30 min repeat flight lines for up to 6 hours to provide a time series for models and to evaluate changes with time of day (illumination, phytoplankton physiology, etc.)
- All data to be processed and distributed over the Web for all users to test and evaluate algorithms and models http://weogeo.coas.oregonstate.edu .

Two Ships and long-term mooring available for Experiment

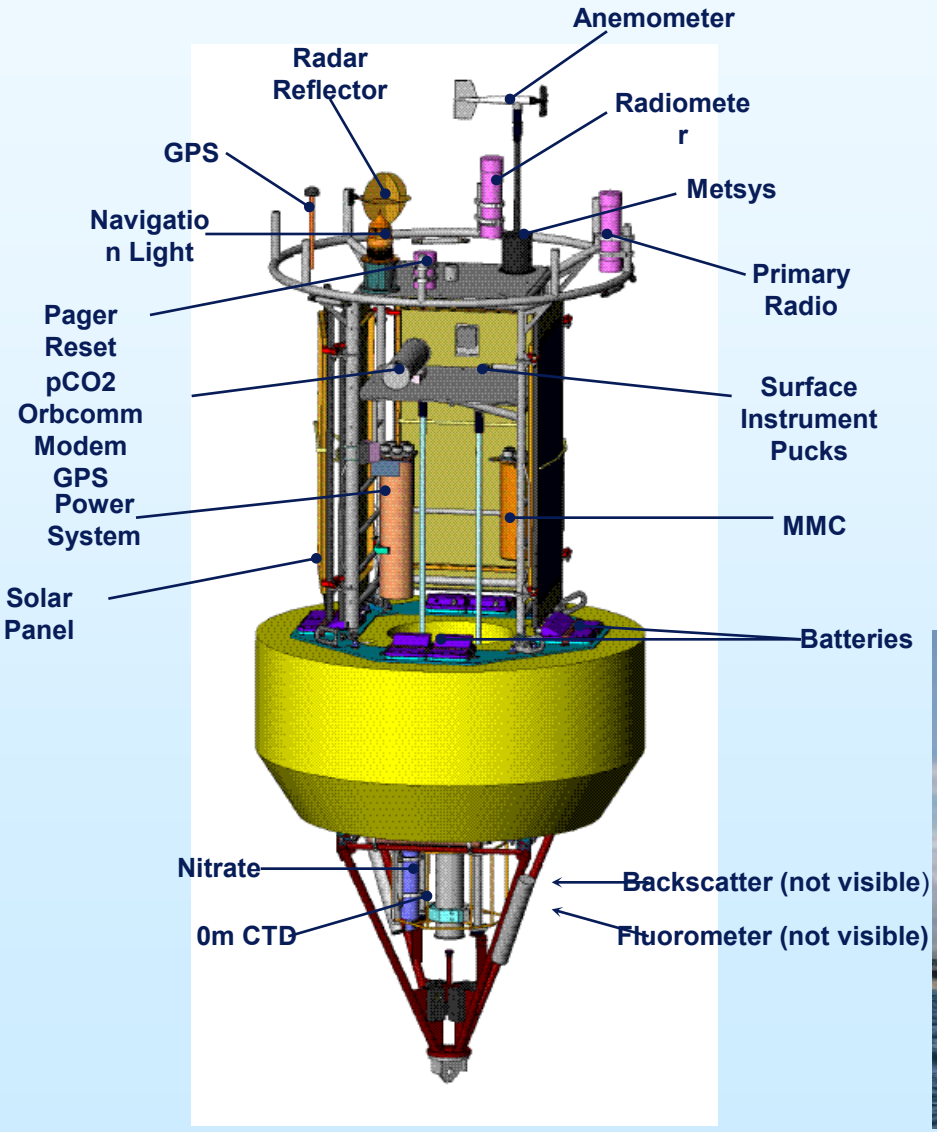

MBARI M-0 mooring

R/V Shana Rae

R/V John H. Martin

A red tide incubator in Monterey Bay?

2002 red tide

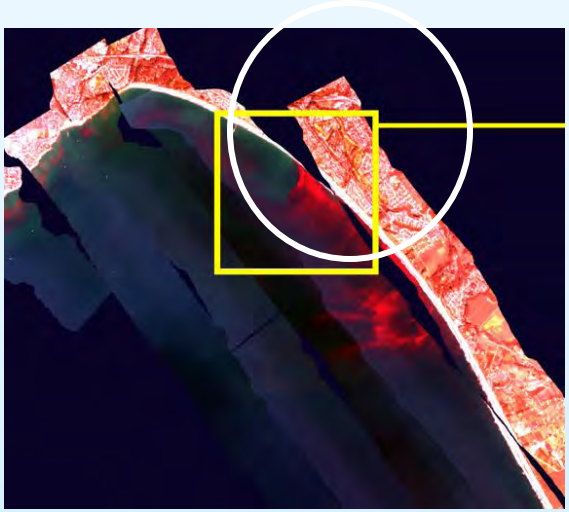

Image from P. Bissett

2004 red tide

R. Kudela, UCSC

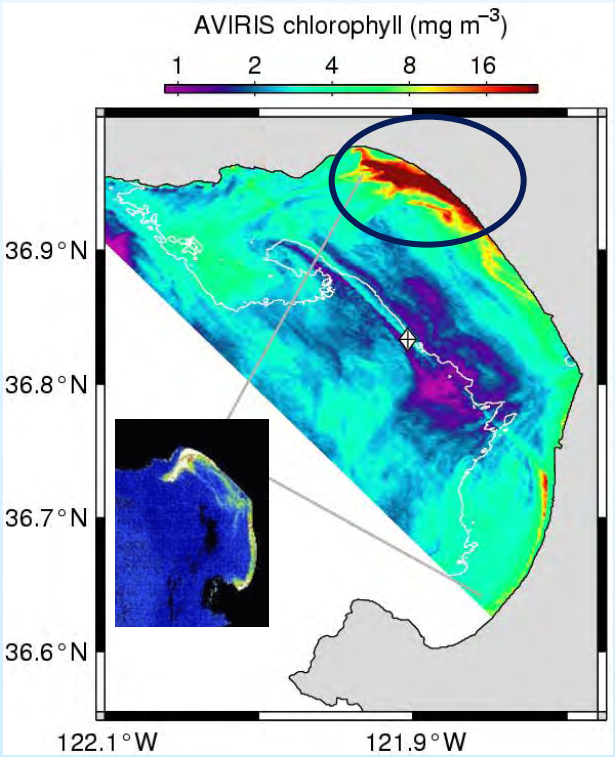

2005 red tide

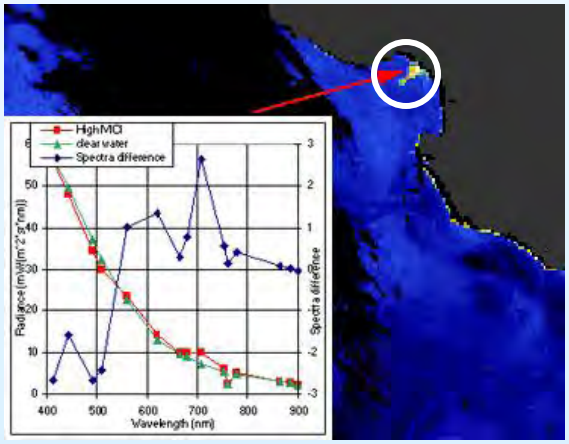

MERIS satellite imagery, 9/17

J. Gower, IOS, Sidney BC

Physical, chemical and biological influences in this region:

- **In the upwelling shadow (stratification)**
- **Downstream of Elkhorn Slough plume (stratification, nutrients, dinoflagellate seed populations)**

September 12, 2006
Grid 03: 10:07 - 10:32

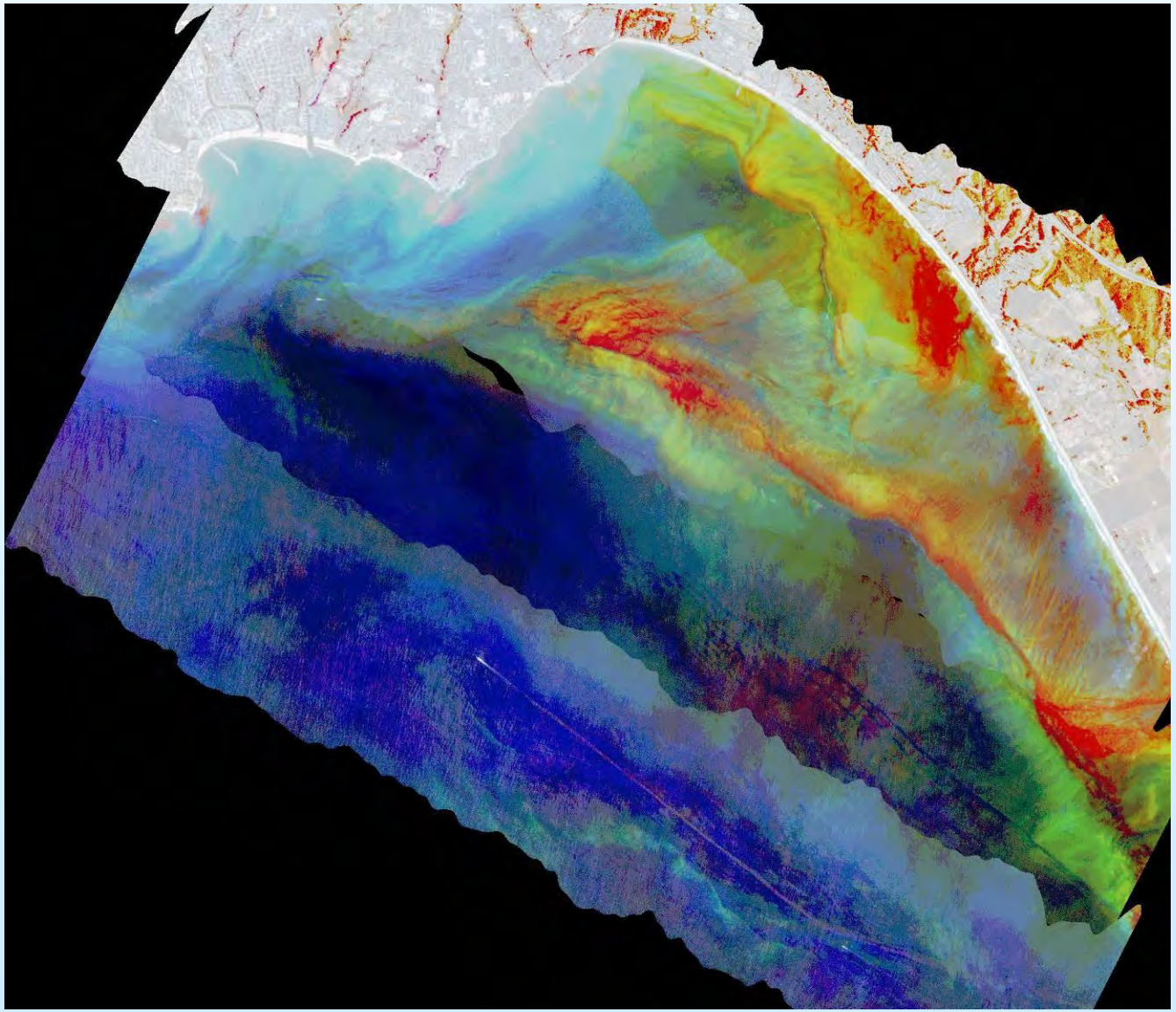

Primary species *Akashiwo sanguinea*

FERI SAMSON data

Bloom disappears on the 15th

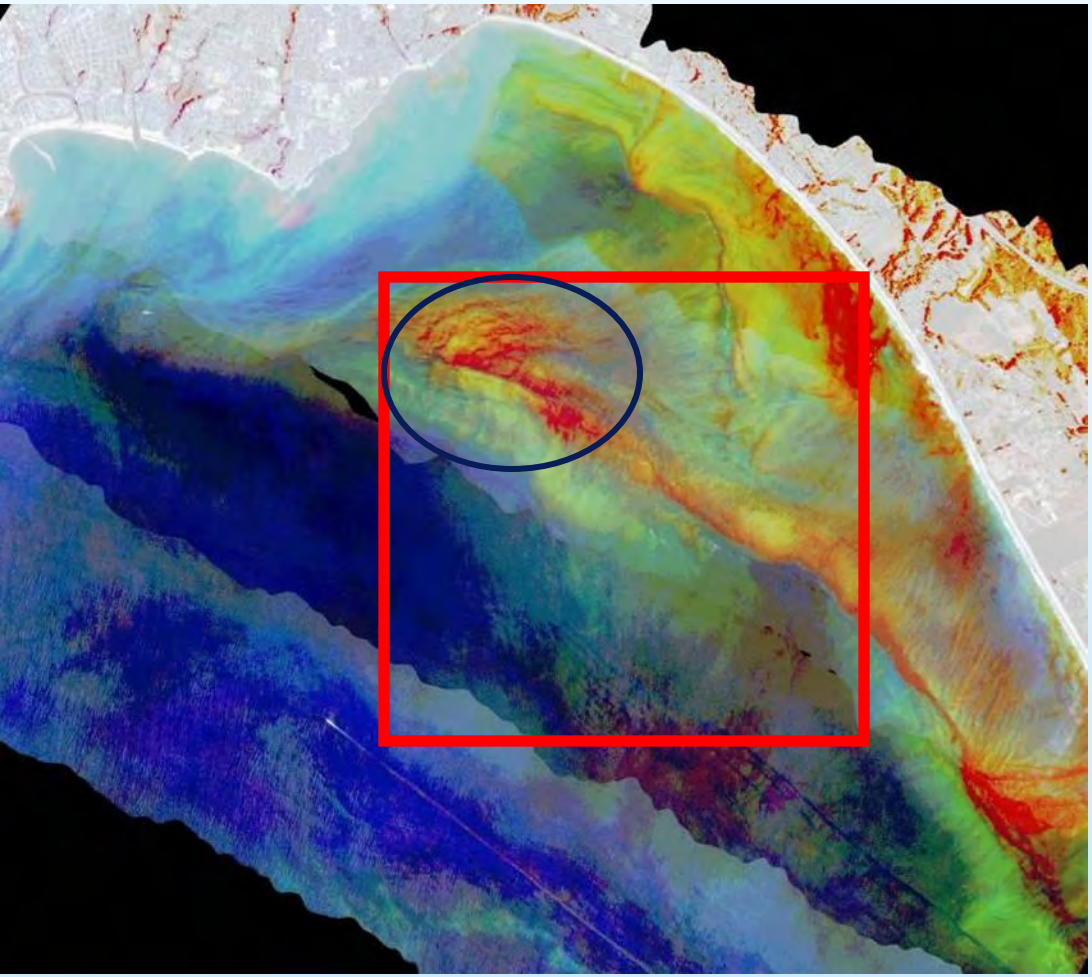

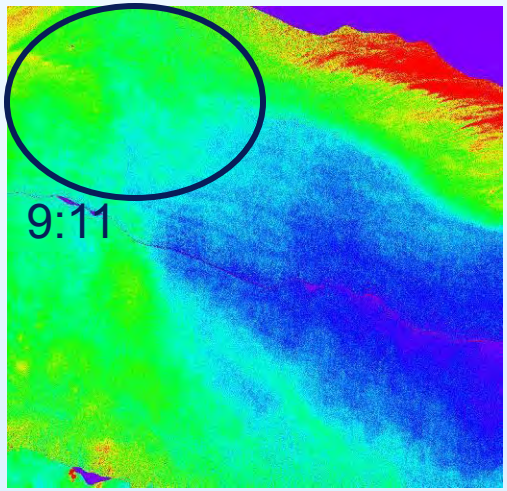

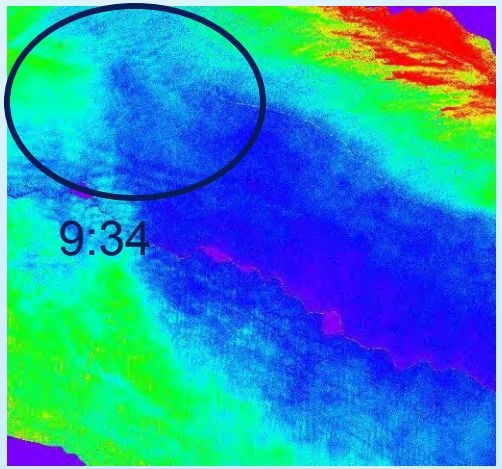

Sept 15, 2006: No bloom
images by Maria Kavanaugh

September 12, 2006 Time sequence of 710 nm: Diurnal migration of the bloom?

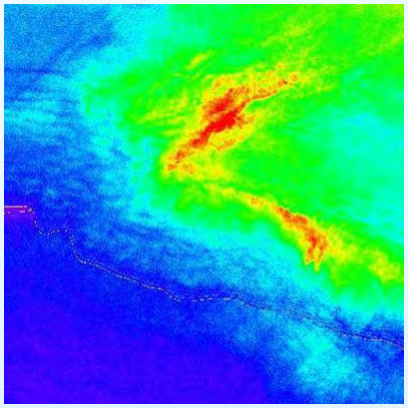

0908

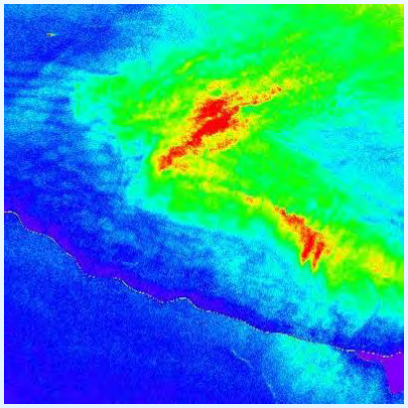

0938

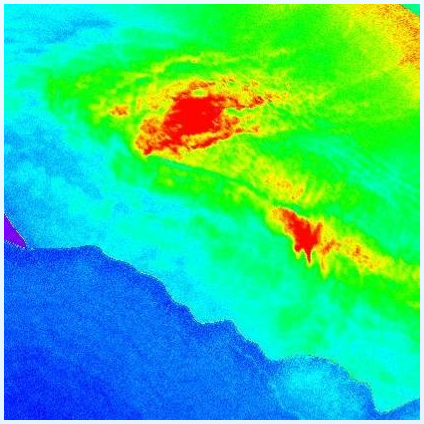

1006

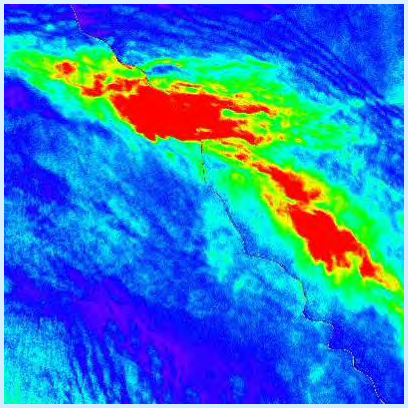

1124

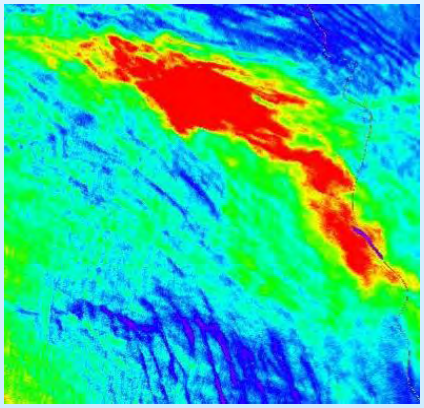

1204

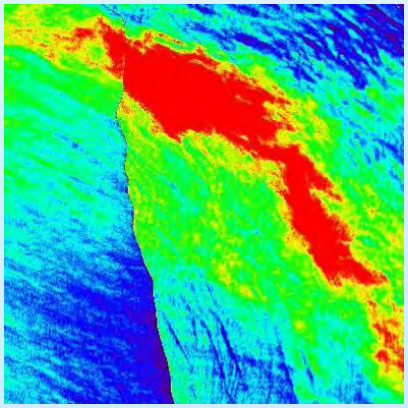

1238

images by Maria Kavanaugh

Dinoflagellates migrate vertically (downward at night). Unique Signature in HES-CW data.

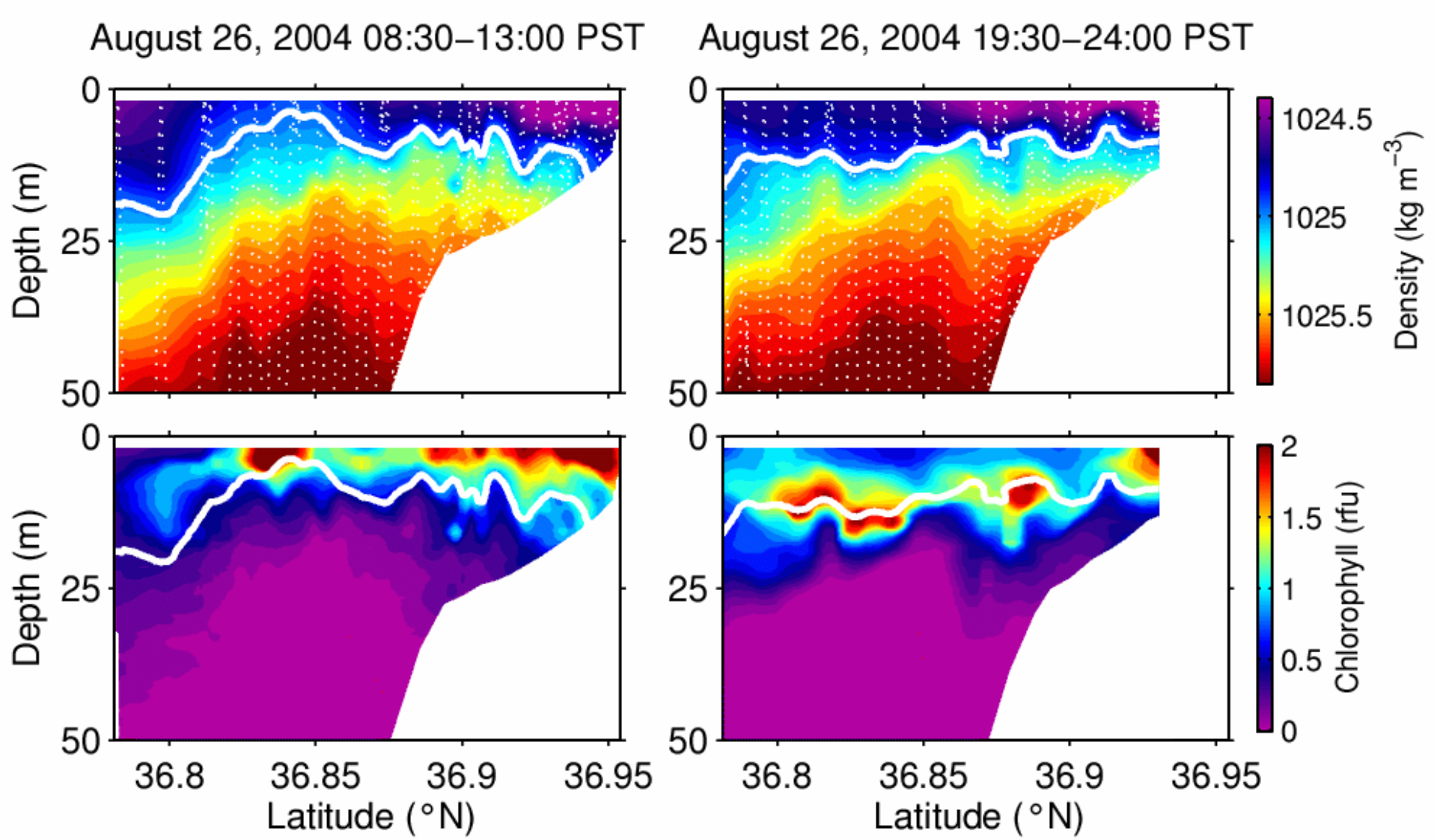

The white contour is the same reference isopycnal in each figure (R. Kudela, UCSC)

Example In-water Optics Data from Bob Arnone, Alan Weidemann and Deric Gray, NRLSSC

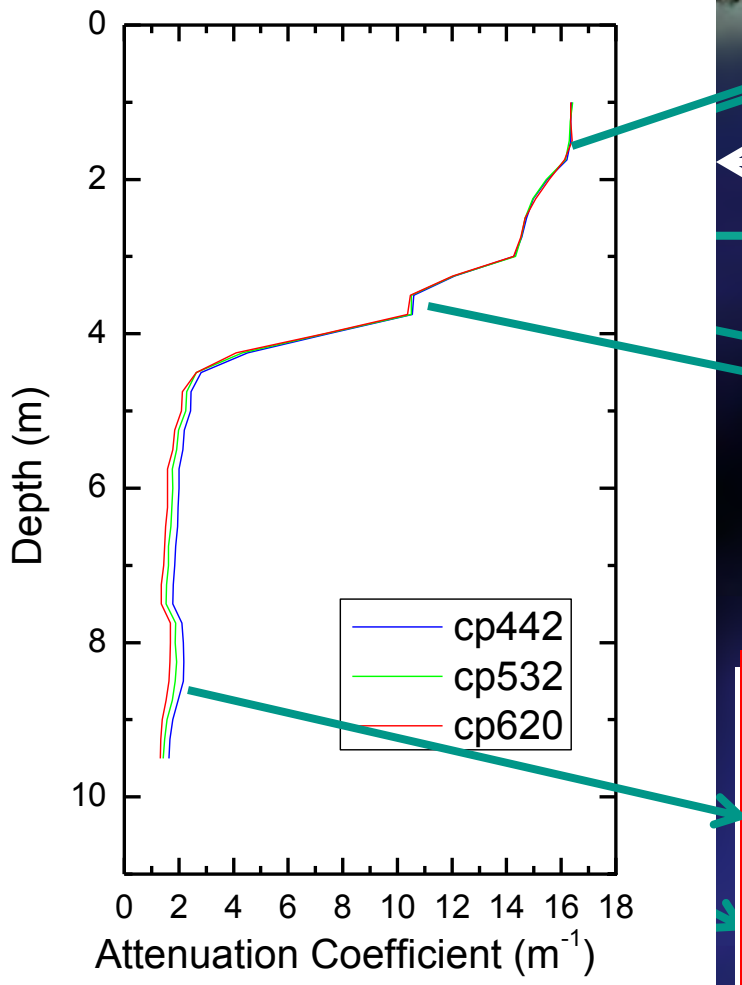

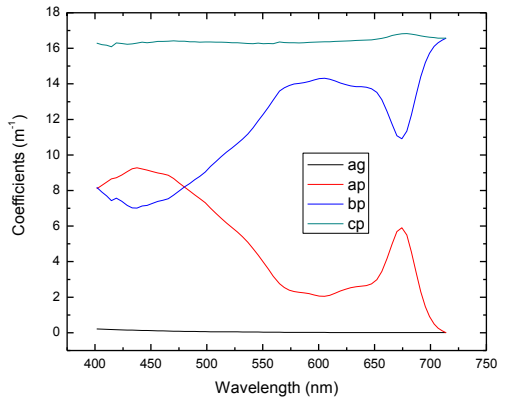

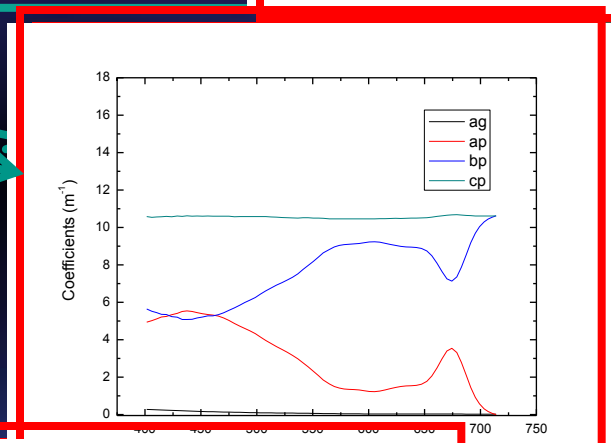

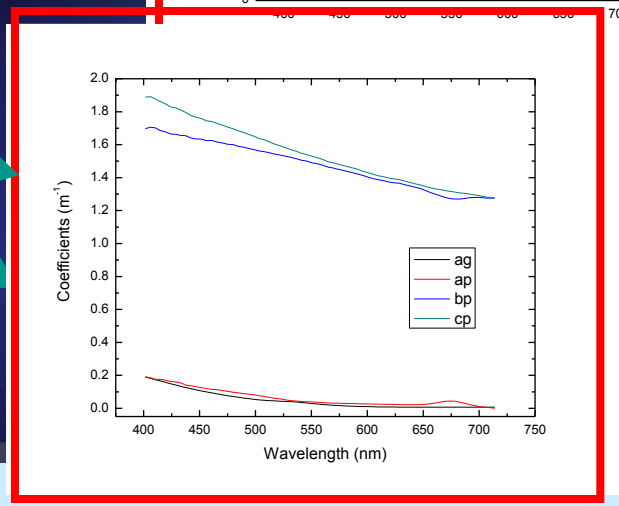

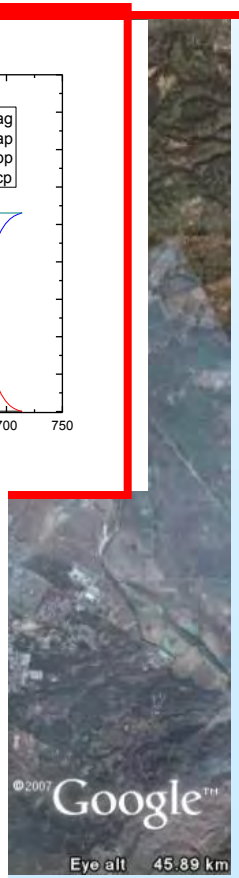

MERIS remote sensing reflectance (Rrs) compared with in situ measurements

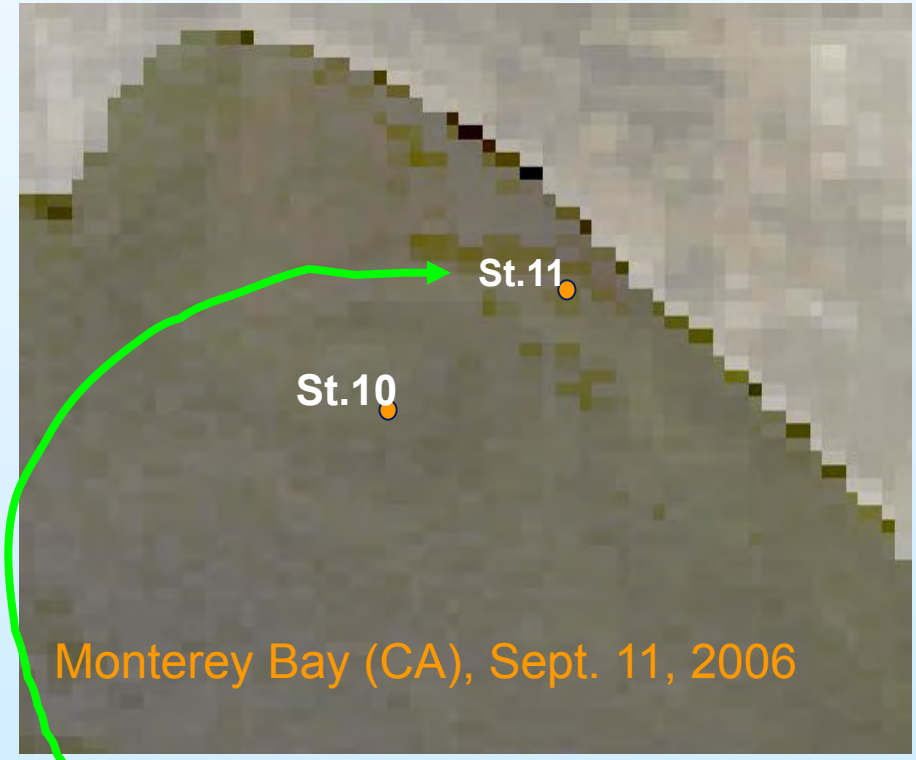

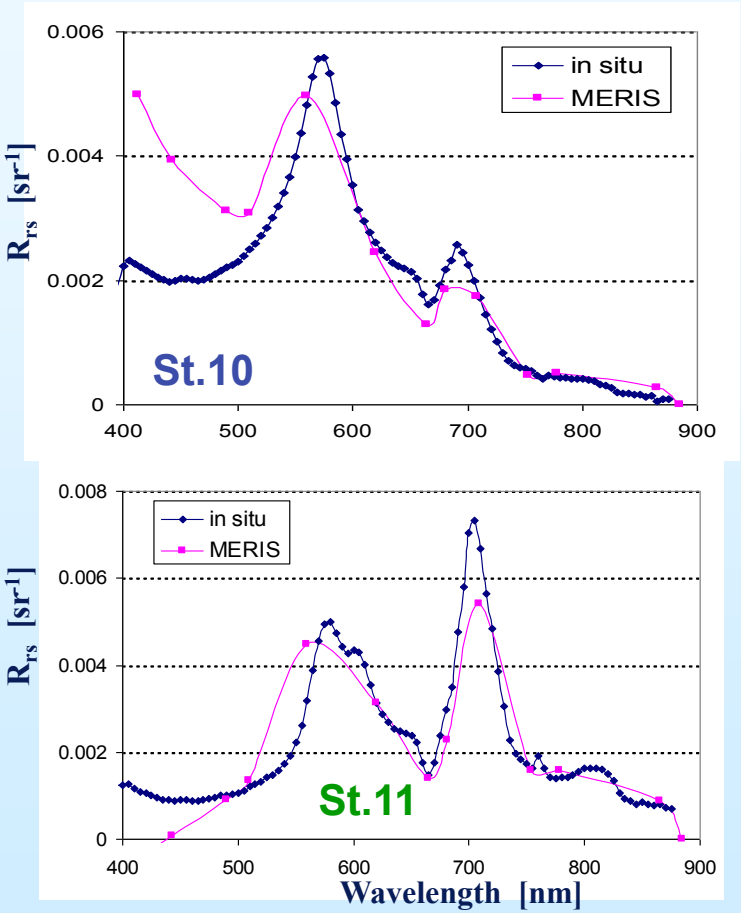

[Chl] was ~ 500 mg/m^3.

Data from Z.-P. Lee, NRLSSC

Heidi M. Sosik: Imaging Flow CytoBot

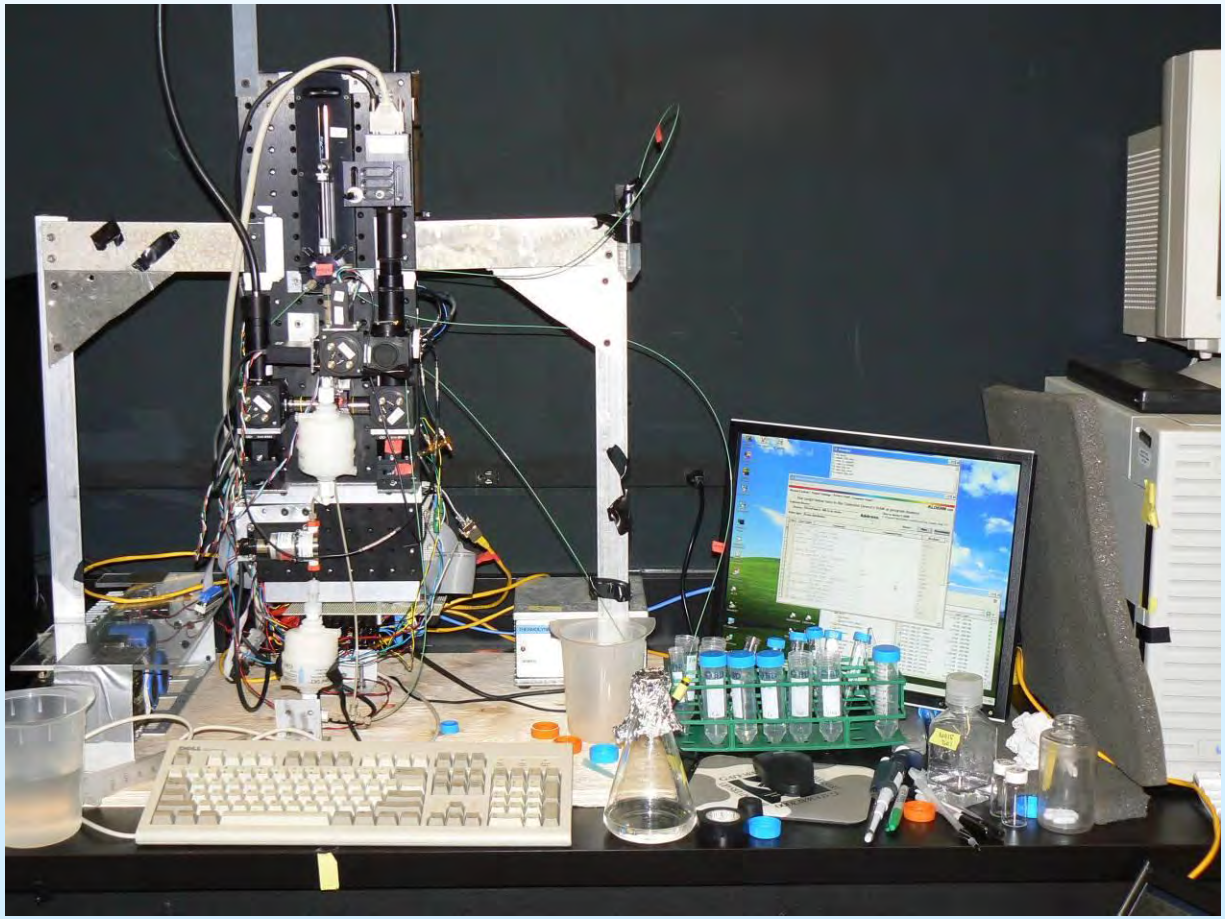

Automated taxonomic classification of phytoplankton sampled with imaging in-flow cytometry, Heidi M. Sosik and Robert J. Olson, Limnol. Oceanogr. Methods (2007) 5:204-216

Data are classified to group

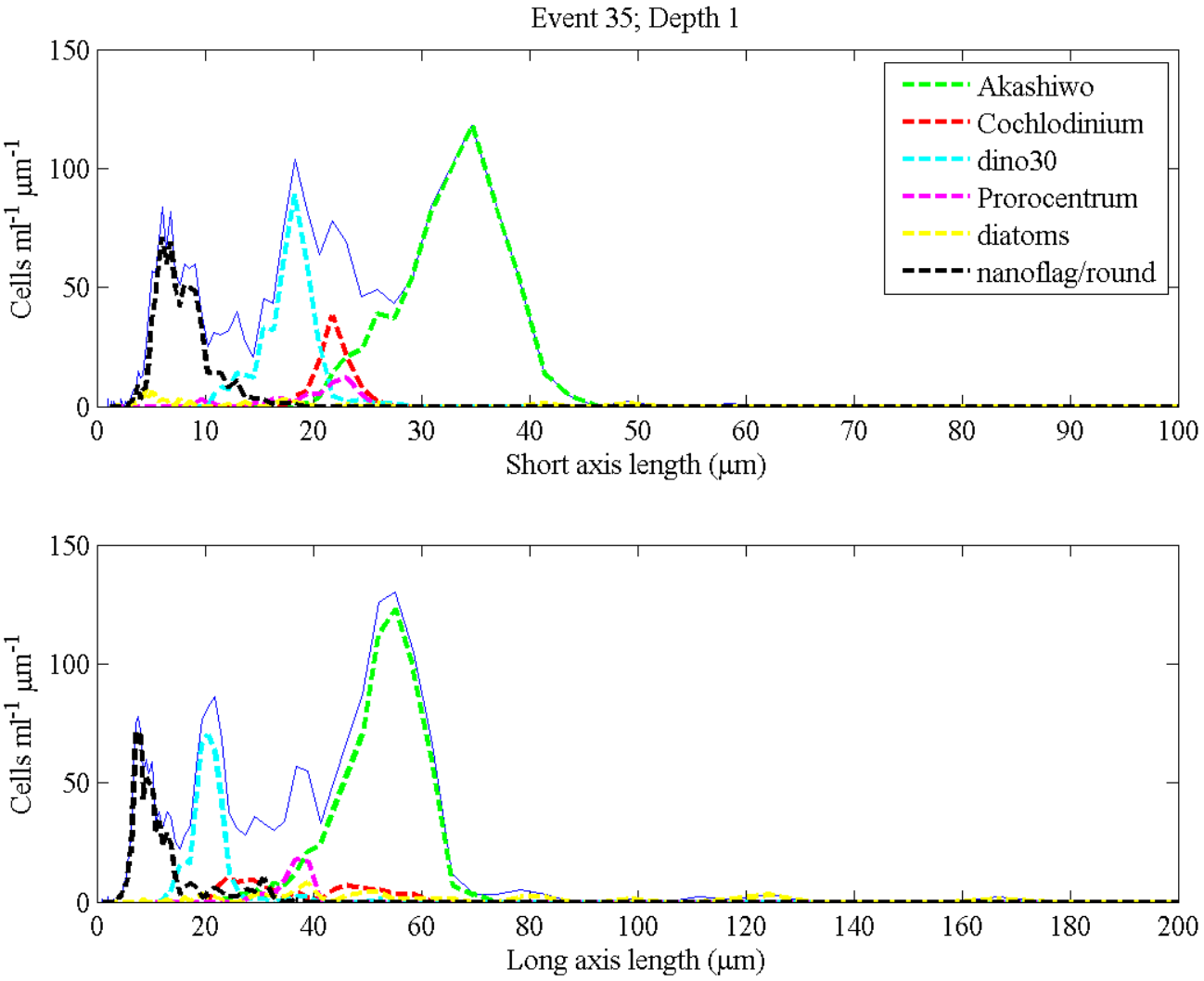

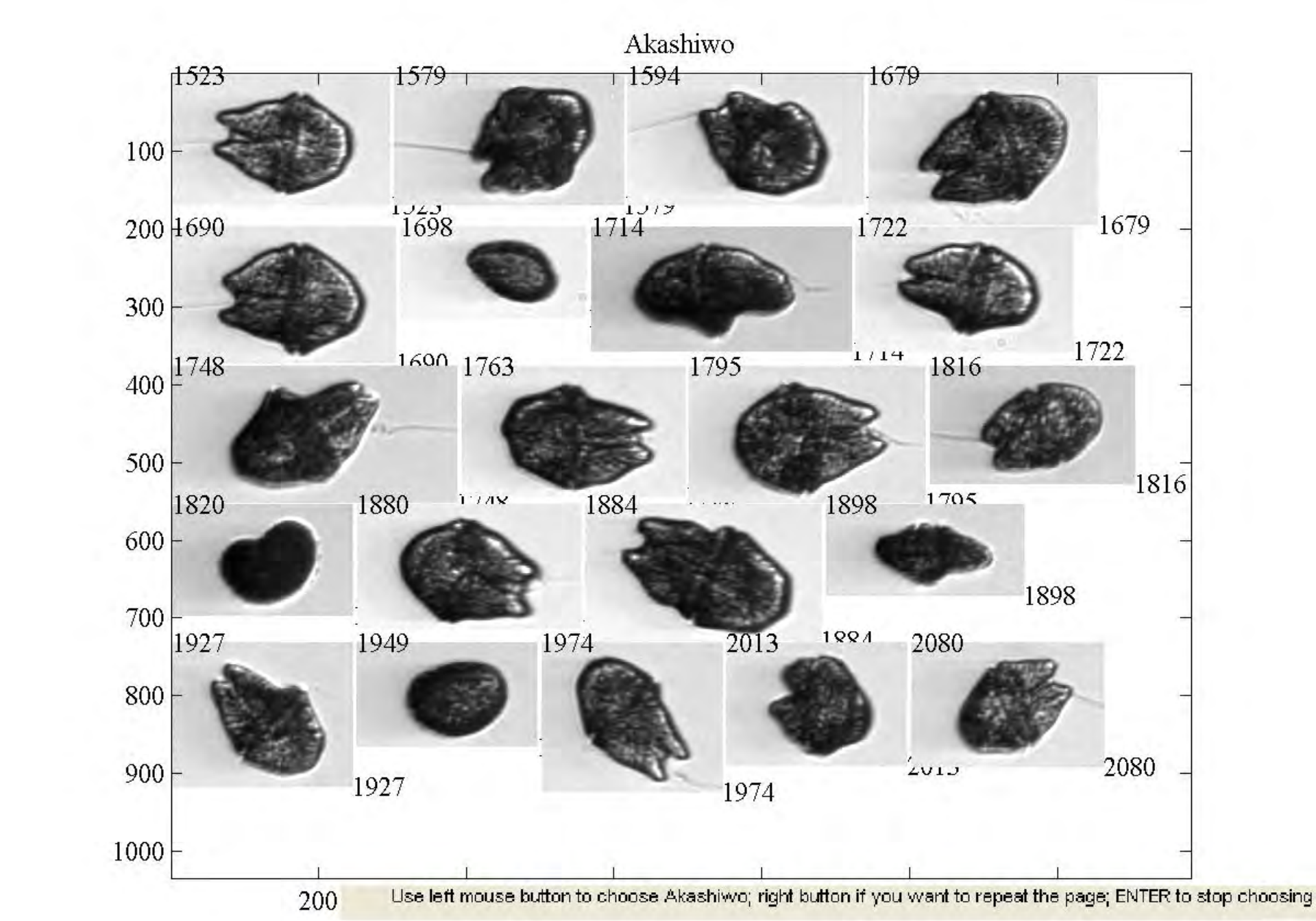
Akashiwo
1523
1579
1594
1679
100
200
1690
1698
1714
1722
1679
300
1748
1763
1795
1816
1722
400
500
1816
1820
1880
1884
1898
600
1898
700
1927
1949
1974
2013
2080
800
900
1927
1974
2080
1000
200
Use left mouse button to choose Akashiwo; right button if you want to repeat the page; ENTER to stop choosing

Monterey Bay Experiment Summary

- Monterey Bay experiment conducted Sept 3-15, 2006.
  - Mid-summer foggy conditions persisted until the last day of the experiment limiting remote sensing opportunities.
- Collected SAMSON Airborne hyperspectral data on Sept 4, 5, 11, 12, and 15.
- Ship data was collected on those dates and additional measurements were made on cloudy days.
- Exceptional data set for characterization of the HAB biology, optics and remote sensing characteristics.
- A dry cold front passed through the area September 15th thoroughly disrupting the HAB.
- Initial analysis of SAMSON data binned to 10 m, 100 m and 300 m (M. Kavanaugh and R. Letelier, OSU, not shown). The 10 m data resolved the HAB patches, binned to 100 m was adequate for most features while 300 m data missed surface HAB patches on the 12th and the general scale of patchiness on the 15th.
- Initial analysis of spectral sampling (Z-P Lee, NRLSSC, not shown) indicates that MERIS channels adequate for sampling this environment.